

Synthesis and Biological Evaluation of Novel 2,4-Diaminoquinazoline Derivatives as *SMN2* Promoter Activators for the Potential Treatment of Spinal Muscular Atrophy

John Thurmond,[†] Matthew E. R. Butchbach,[‡] Marty Palomo,[†] Brian Pease,[†] Munagala Rao,[†] Louis Bedell,[†] Monica Keyvan,[†] Grace Pai,[†] Rama Mishra,[†] Magnus Haraldsson,[§] Thorkell Andresson,[§] Gisli Bragason,[§] Margret Thosteinsdottir,[§] Jon Mar Bjornsson,[§] Daniel D. Coover,[‡] Arthur H. M. Burghes,[‡] Mark E. Gurney, and Jasbir Singh^{*,†}

deCODE chemistry, Inc., 2501 Davey Road, Woodridge, Illinois 60517, deCODE genetics, Inc., Sturlugata 8, IS-101, Reykjavik, Iceland, Department of Molecular and Cellular Biochemistry, College of Medicine and Public Health, The Ohio State University, Columbus, Ohio 43210

Received December 23, 2006

Proximal spinal muscular atrophy (SMA) is an autosomal recessive disorder characterized by death of motor neurons in the spinal cord that is caused by deletion and/or mutation of the survival motor neuron gene (*SMN1*). Adjacent to *SMN1* are a variable number of copies of the *SMN2* gene. The two genes essentially differ by a single nucleotide, which causes the majority of the RNA transcripts from *SMN2* to lack exon 7. Although both *SMN1* and *SMN2* encode the same Smn protein amino acid sequence, the loss of *SMN1* and incorrect splicing of *SMN2* have the consequence that Smn protein levels are insufficient for the survival of motor neurons. The therapeutic goal of our medicinal chemistry effort was to identify small-molecule activators of the *SMN2* promoter that, by up-regulating gene transcription, would produce greater quantities of full-length Smn protein. Our initial medicinal chemistry effort explored a series of C5 substituted benzyl ether based 2,4-diaminoquinazoline derivatives that were found to be potent activators of the *SMN2* promoter; however, inhibition of DHFR was shown to be an off-target activity that was linked to ATP depletion. We used a structure-guided approach to overcome DHFR inhibition while retaining *SMN2* promoter activation. A lead compound **11a** was identified as having high potency ($EC_{50} = 4$ nM) and 2.3-fold induction of the *SMN2* promoter. Compound **11a** possessed desirable pharmaceutical properties, including excellent brain exposure and long brain half-life following oral dosing to mice. The piperidine compound **11a** up-regulated expression of the mouse *SMN* gene in NSC-34 cells, a mouse motor neuron hybrid cell line. In type I SMA patient fibroblasts, compound **11a** induced Smn in a dose-dependent manner when analyzed by immunoblotting and increased the number of intranuclear particles called gems. The compound restored gems numbers in type I SMA patient fibroblasts to levels near unaffected genetic carriers of SMA.

Introduction

Spinal muscular atrophy (SMA) is characterized by degeneration of motor neurons in the anterior horn of the spinal cord, atrophy of skeletal muscle, and consequent weakness. SMA afflicts approximately 1 in 6000–8000 newborns and is the leading hereditary cause of mortality in infants.^{1,2} The carrier frequency for SMA is about 1 in 40 individuals.^{2,3} SMA is classified into four types (types I–IV) according to age of onset and severity of disease. Type I (acute, also called Werdnig–Hoffmann disease) SMA typically presents itself within 6 months after birth; children never sit or stand and usually die before the age of 2 without respiratory intervention. Type II (intermediate) SMA patients have an onset after 6 months of age and are usually diagnosed by 15 months. These children may learn to sit but cannot stand or walk. Type III (mild) SMA, often referred to as Kugelberg–Welander disease or juvenile spinal muscular atrophy, is usually diagnosed between 2 and 17 years of age. These patients are able to sit and walk but often become wheelchair-bound as the course of disease progresses. Type IV SMA patients (adult form of SMA) are characterized by age of onset at >30 years and show very mild signs of muscle weakness.

SMA is caused by mutation or homozygous deletion of the telomeric copy of the survival of motor neuron gene (*SMN1*) on chromosome 5q13.⁴ A second, duplicated copy of the gene, designated as *SMN2*, is found adjacent on chromosome 5 in the direction of the centromere.⁴ The transcripts arising from the *SMN1* gene are spliced correctly to yield full-length Smn mRNA. In contrast, a translationally silent single nucleotide mutation (C → T) in exon 7 of the *SMN2* gene leads to missplicing of the *SMN2* mRNA, deleting exon 7 from 80% to 90% of *SMN2* transcripts (termed the $\Delta 7$ form).^{4–6} Only ~10–20% of *SMN2* gene transcripts correctly splice to produce full-length mRNA.^{4–8} The absence of exon 7 from the *SMN2* mRNA results in the synthesis of truncated Smn protein with reduced ability for self-oligomerization, causing instability and degradation of the protein.^{9,10} Therefore, SMA patients, who lack the *SMN1* gene, have low (full-length) Smn protein levels that are insufficient for motor neuron survival.^{11,12}

The severity of SMA disease correlates with the number of *SMN2* gene copies present in the affected child. The copy number of the human *SMN2* gene varies in the general population and therefore the corresponding amount of full-length Smn protein produced from these genes.^{3,13–15} The correlation is not absolute because it is important to consider the number of intact *SMN2* genes and how much Smn protein the particular *SMN2* gene produces.^{15,16} In mice there is only one *SMN* gene^{17,18} that is equivalent to *SMN1*. Homozygous deletion of the single mouse *SMN* gene results in embryonic lethality.¹⁹ A similar situation most likely exists in humans because no individual entirely lacking *SMN* genes has been reported, but

* To whom correspondence should be addressed. Phone: 630-783-4915. Fax: 630-783-4646. E-mail: jsingh@decode.com.

[†] deCODE chemistry, Inc.

[‡] The Ohio State University.

[§] deCODE genetics, Inc.

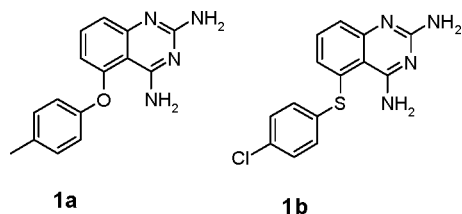


Figure 1. HTS hits.³³

chromosomes lacking *SMN* genes do exist. In addition, deleting the mouse *SMN* gene in a specific tissue causes destruction of that specific cell type, again indicating *SMN* is an essential gene.^{20–22} To rescue the embryonic lethality, *SMN2* transgenes have been introduced into *SMN* null mice, and indeed, two copies of *SMN2* result in severe SMA whereas eight copies result in rescue of phenotype.^{23–25} Clearly, expression of full length *Smn* at the right time can rescue the SMA phenotype in mice. In addition, overexpression of the *Smn* form lacking exon 7 is not harmful but beneficial to the SMA phenotype.²⁶ Expression of a mild missense mutation on the severe SMA background results in mild SMA mice.²⁷ Therefore, a therapeutic agent that increases human *SMN2* gene expression and consequent production of (full-length) *Smn* protein has the potential to reduce the clinical severity of SMA.

The therapeutic goal of increasing the level of *Smn* protein might be achieved by (i) enhancing *SMN2* gene transcription or (ii) suppressing defective splicing of the *SMN2* mRNA, thereby increasing the number of full-length transcripts, or alternatively a combination of steps i and ii. Small-molecule activators of the *SMN2* gene promoter, which enhance *Smn* expression, thus represent a promising strategy for the treatment of SMA. A series of compounds such as butyrate, 4-phenylbutyrate, valproate, and aclarubicin have been reported to increase *Smn*.^{28–32} However, these compounds need to be used at high concentration, have poor metabolic properties, are relatively nonspecific, or have toxicity problems.

A cell-based assay for *SMN2* promoter activation and the details of an ultra-high-throughput screening (uHTS) campaign of 558 000 compounds were described by Jarecki et al.³³ This effort led to the identification of several small-molecule hits representing nine scaffolds.³³ The quinazoline-based compounds **1a** and **1b** (Figure 1) were among the most potent hits from the uHTS campaign. When tested on fibroblasts derived from SMA type I patients, these compounds increased the relative abundance of the full-length *SMN* transcript, increased *Smn* protein levels, and increased the numbers of intranuclear structures containing *Smn*, termed gems or Cajal bodies. Gems are intranuclear concentrations of *Smn* found in most cells. *Smn* functions in the assembly of small nuclear ribonucleoprotein or snRNPs, which are important for splicing exons to create mRNA. On the basis of our analysis of the chemical tractability of the different uHTS hit series and given that the quinazoline-based hits also possessed the attributes mentioned above, we selected the quinazoline scaffold for SAR exploration. In this paper, we describe the SAR and lead optimization of quinazoline based activators of the *SMN2* promoter. This has led to the development of a series of 2,4-diaminoquinazoline analogues with high potency in the cell-based *SMN2* promoter assay, the ability to activate the endogenous mouse *SMN* gene, oral bioavailability, permeability across the blood–brain barrier,

good pharmacokinetic properties, and an increase in gems numbers in cultured type I SMA patient fibroblasts.

Chemistry

The 2,4-diaminoquinazoline derivatives functionalized at the C5 position were prepared via cyclization of 6-substituted 2-aminobenzonitriles with chloroformamidinium hydrochloride in diglyme.³⁴ The 6-substituted 2-nitrobenzonitriles were prepared by displacement of one of the nitro groups in 2,6-dinitrobenzonitrile. Reduction of the 6-substituted 2-nitrobenzonitrile to 6-substituted 2-aminobenzonitrile was accomplished using iron powder in hydrochloric acid. Alternatively, a more efficient approach starting from 2,6-difluorobenzonitrile (**2**), analogous to the procedure reported by Hynes,³⁵ was utilized to prepare 5-substituted 2,4-diaminoquinazolines **1**, **5–9**, and **11–13** as outlined in Scheme 1. Reaction of 2,6-difluorobenzonitrile (**2**) with a wide variety of alcohols (aryl or heteroarylmethyl alcohols; primary, secondary, or tertiary alkyl alcohols; α -alkylarylmethyl alcohols, bicyclic secondary alcohols; and piperidine methanol) (**3**) provided 2-fluoro-6-(aryloxy/phenoxy)benzonitriles (**4**). Cyclization of 2-fluoro-6-(aryloxy/phenoxy)benzonitriles (**4**) to the corresponding 5-substituted 2,4-diaminoquinazolines **1**, **5–9**, and **11–13** was achieved by heating with guanidine carbonate in *N,N*-dimethylacetamide (Scheme 1). The alcohols used for reaction with **2** were either obtained from commercial sources or prepared as outlined in Schemes 2–4.

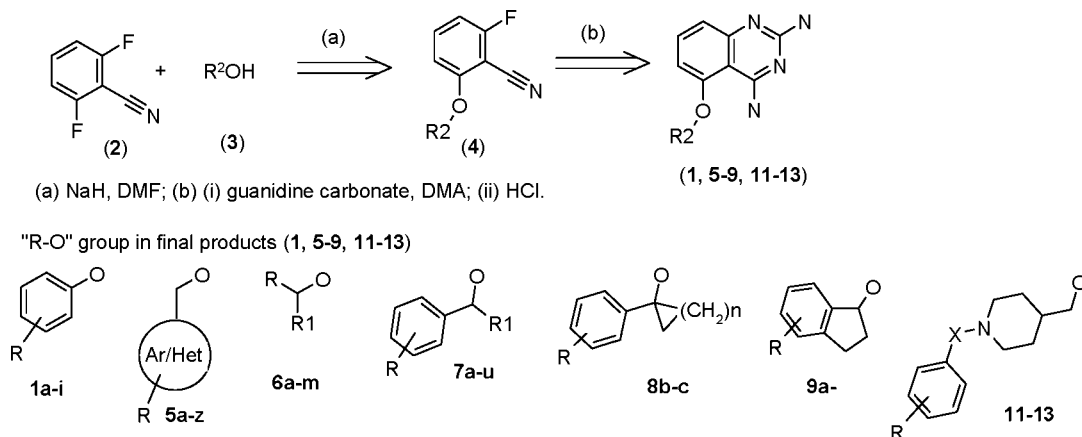
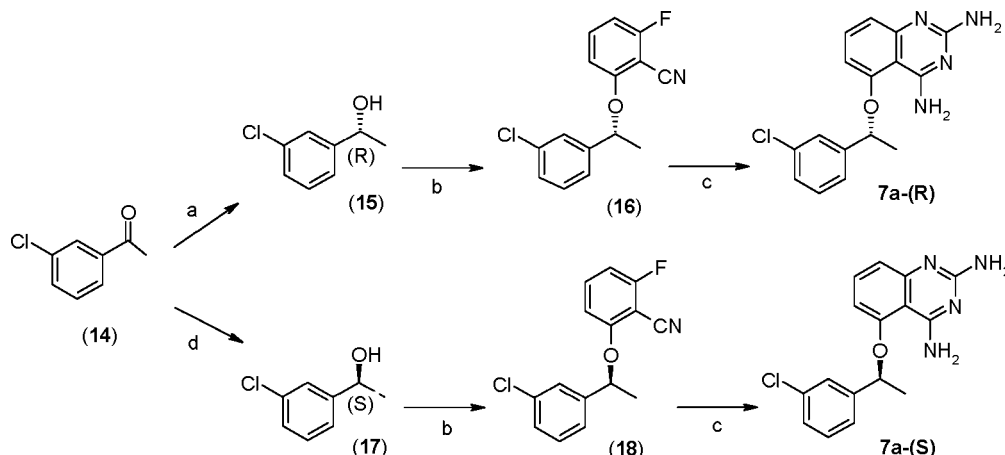
Reduction of ketones **14** with a chiral reducing agent³⁶ in either catalytic or equimolar amounts of a chiral reagent provided alcohols **15** and **17** of known chirality with very high % ee (Scheme 2). Reaction of the chiral alcohols **15** and **17** with 2,6-difluorobenzonitrile followed by cyclization with guanidine carbonate yielded the chiral 5-substituted quinazolines with known chirality. The enantiomeric purity of the final products (5- α -methylaryloxy 2,4-diaminoquinazolines (*R*)-**7a** and (*R*)-**7u**, and (*S*)-**7a** and (*S*)-**7u**) was determined by chiral HPLC (see Experimental section).

Cyclic tertiary alcohols (**20b,c**) were prepared by addition of 3-chlorophenylmagnesium bromide to the corresponding cyclic ketone (**19b,c**) (Scheme 3). These tertiary alcohols were converted to the target products **8a–c** using procedures outlined in Scheme 1. The substituted 1-indanols (**23**) were prepared by intramolecular cyclization of the phenyl substituted phenethyl acid chloride (**21**) followed by reduction of the resulting 1-indanones (**22**, Scheme 4). 1-Indanols were reacted with **2** followed by cyclization of the corresponding intermediate **4** to furnish the quinazoline analogues **6a,b**.

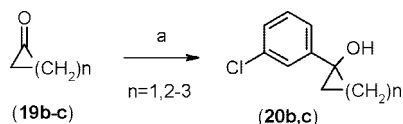
Reverse benzyl analogues **10a–k** were prepared from 2-bromomethyl-6-nitrobenzonitrile (Scheme 5). Substituted phenols were reacted with 2-bromomethyl-6-nitrobenzonitrile **24** in the presence of potassium carbonate to form the respective phenoxynitrobenzonitriles **25**. The nitro group was reduced with stannous chloride to provide aminobenzonitrile **26**. Guanidine hydrochloride was used for the cyclization reaction to afford quinazoline derivatives **10a–k**.

N-Substituted piperidine methyl ether derivatives were prepared by functionalization of the piperidine nitrogen either following the cyclization step to form quinazoline (route A) or prior to quinazoline ring formation (route B). Route A was amenable to parallel synthesis. It provided for rapid SAR studies. For route A, the fluorobenzonitrile intermediate **29** was cyclized to form the quinazoline ring. Subsequent BOC deprotection provided the free piperidine derivative **31**. This key intermediate was reacted with benzyl halides, acid chlorides, and sulfonyl

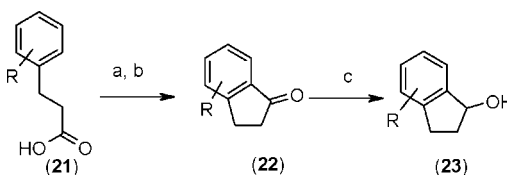
Scheme 1

Scheme 2^a

^a Reagents: (a) borane-THF, (*S*)-MeCBS; (b) NaH, DMF, **2**; (c) guanidine carbonate, DMA; (d) borane-THF, (*R*)-MeCBS.

Scheme 3^a

^a Reagents: (a) 2-Chlorophenylmagnesium bromide, THF.

Scheme 4^a

^a Reagents: (a) SOCl₂; (b) AlCl₃; CH₂Cl₂; (c) NaBH₄, MeOH.

chlorides to yield **11**, **12**, and **13**, respectively. 4-Piperidinemethanol was BOC-protected using di-*tert*-butyl dicarbonate in dichloromethane. Subsequently, alcohol **28** was coupled to 2,6-difluorobenzonitrile to provide compound **29**. For route B, the

BOC group was deprotected to give intermediate **32**. It was reacted with acid chlorides, sulfonyl chlorides, and benzyl halides to give the N-functionalized piperidine intermediate **33**. 6-Substituted 2-fluorobenzonitrile **33x** was further cyclized with guanidine carbonate to yield 5-substituted 2,4-diaminoquinazolines **11–13** (Scheme 6). This route was used for scale up of selected analogues for generation of samples for PK studies.

Results and Discussions

uHTS Hits. Following the uHTS campaign described by Jarecki et al.³³ and before starting the focused medicinal chemistry program, screening hits were resynthesized or obtained from commercial sources. Their identity was confirmed by NMR, LC/MS, HPLC, and elemental analysis, whenever appropriate. Retesting of hits **1a–d**, (Table 1) in the NSC-34 SMN2 promoter assay verified that the EC₅₀ obtained in our assays compared well ($r^2 = 0.98$) with the corresponding data reported by Jarecki et al.³³

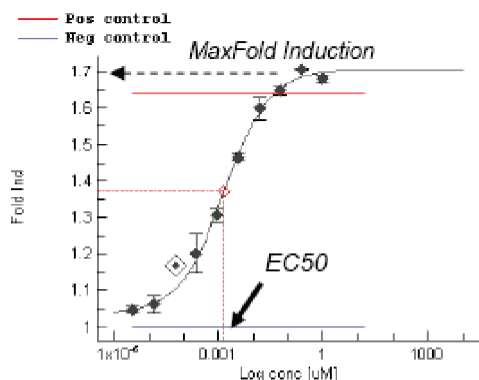
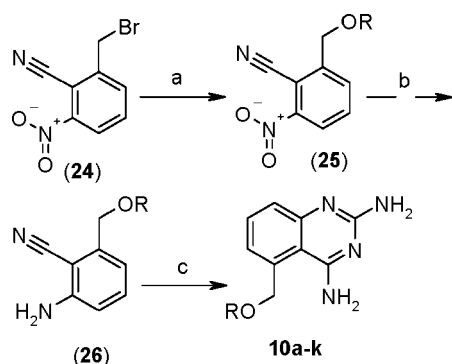
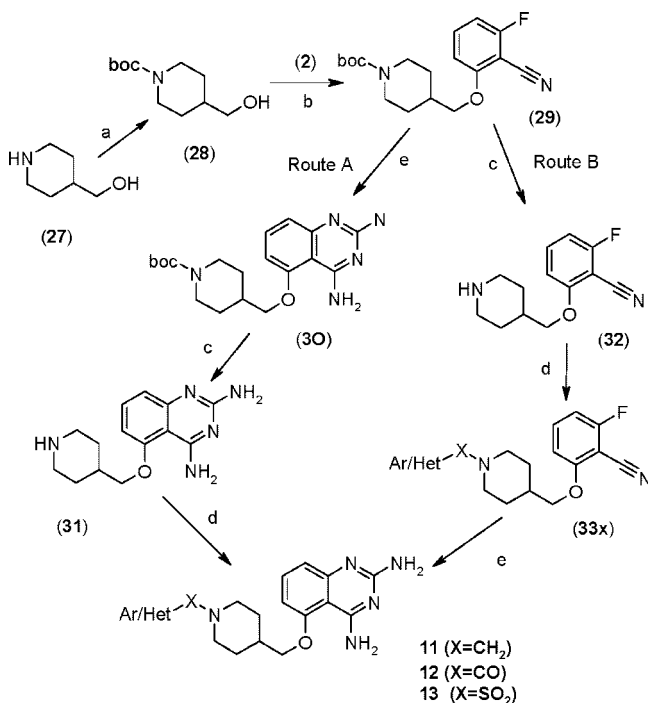


Figure 2. Example of dose-response curve and key assay parameters.

Scheme 5^a

^a Reagents: (a) K_2CO_3 , ROH; (b) $SnCl_2$, HCl; (c) chloroformamidine hydrochloride, diglyme.

Scheme 6^a

^a Reagents: (a) $(BOC)_2O$, TEA, CH_2Cl_2 ; (b) NaH, DMF; (c) HCl/*p*-dioxane; (d) acid chloride, sulfonyl chloride, or benzyl halide, base; (e) guanidine carbonate, DMA.

A sample dose–response curve for *SMN2* promoter induction in NSC-34 cells is shown in Figure 2. Two parameters used to drive our SAR studies were (i) “ EC_{50} ” value, reflecting potency of a compound, and (ii) “MaxFoldInd” (MFI), referring to the maximum observed efficacy for a promoter induction compared to nonactivated cells. Both EC_{50} and maximum fold induction (MFI) are highlighted for illustration in Figure 2. Lead optimization was expected to provide maximum fold induction at low (EC_{50}) concentration. Therefore, for generating a robust SAR, we were optimizing both parameters.

SAR of C5-OAr and C5-OCH₂Ar. In addition to previously reported³³ tolyloxy analogue **1a**, we initially prepared several additional 5-aryloxyquinazoline analogues. As shown in Table 1, all of the substituted phenyl **1a–f** and heteroaromatic **1g–i** analogues showed submicromolar to micromolar EC_{50} , chloro analogues **1e** and **1f** being the best (EC_{50} = 0.52 and 0.48 μ M, respectively). Thioether analogue **1b** and the corresponding sulfoxide and sulfone were also prepared. Thioether **1b** featured EC_{50} = 0.22 μ M, whereas the corresponding sulfone showed a

Table 1. Activity of C5-O-Aryl Analogues in the *SMN2* Promoter Assay

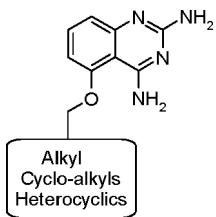
compd	Ar	EC_{50} (SD), μ M	MaxFoldInd
1a	4-Me phenyl	1.21	1.6
1c	4-Cl phenyl	2.06(0.67)	1.84
1d	4-F phenyl	1.32	1.7
1e	2-Cl phenyl	0.51(0.05)	1.76
1f	3-Cl phenyl	0.48(0.35)	1.74
1g	1-(5-isoquinoline)	1.03(0.71)	2.04
1h	2-(5-isoquinoline)	1.26(1.34)	2.3
1i	1-(8-isoquinoline)	2.44(0.58)	1.59

Table 2. Activity of C5-O-CH₂-Aryl Analogues in the *SMN2* Promoter Assay

compd	Ar	EC_{50} (SD), μ M	MFI
5a	2-Cl phenyl	0.14(0.04)	2.0
5b	3-Cl phenyl	0.078(0.03)	1.74
5c	4-Cl phenyl	0.18(0.1)	1.84
5d	2-Me phenyl	0.28	1.6
5e	3-Me phenyl	0.12	1.7
5f	4-Me phenyl	0.22	2.04
5g	2-F phenyl	0.052(0.04)	2.3
5h	3-F phenyl	0.055(0.01)	1.59
5i	4-F phenyl	0.053(0.04)	1.8
5j	2-OMe phenyl	0.065(0.04)	1.6
5k	3-OMe phenyl	0.066(0.04)	1.6
5l	4-OMe phenyl	0.30(0.23)	1.7
5m	2-CF ₃ phenyl	0.016(0.01)	1.6
5n	3-CF ₃ phenyl	0.023(0.02)	1.5
5o	4-CF ₃ phenyl	0.017(0.01)	1.6
5p	3,5-F ₂ phenyl	0.014(0.01)	1.9
5q	3,4-F ₂ phenyl	0.014(0.01)	1.8
5r	2,5-F ₂ phenyl	0.047(0.03)	2.0
5s	2,4-F ₂ phenyl	0.12(0.06)	1.8
5t	2,6-F ₂ phenyl	0.19(0.05)	1.8
5u	2-Py	0.25(0.01)	1.9
5v	3-Py	0.024(0.01)	2.1
5w	2-thiophenyl	0.073(0.02)	1.9
5x	2-furanyl	0.30(0.2)	1.7
5y	3-(5-methylisoxazolyl)	0.28(0.09)	2.2
5z	3-(1-isoquinoline)	0.22(0.06)	2.3

10-fold loss in activity (EC_{50} = 2.4 μ M). The respective sulfoxide was inactive.³⁷

In order to explore expanded conformational space and the electronic nature of the putative binding pocket around C5 substituents, a series of 5-benzyloxy analogues were prepared. As shown in Table 2, benzyloxy analogues provided a significant improvement of promoter activity compared to the corresponding phenoxy series (see, for example, **1f** vs **5b**, **1c** vs **5c**, and **1d** vs **5i**). For the benzyloxy series, incorporation of halogen and alkyl substituents enhanced promoter activity. The observed activity pattern for halogen

Table 3. Activity of C5-O-CH₂-Non-Aryl Analogues in the SMN2 Promoter Assay


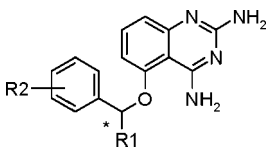
compd	non-aryl	EC ₅₀ (SD), μ M	MaxFoldInd
6a	Me	0.17(0.04)	2.1
6b	Et	0.18(0.04)	2.1
6c	<i>n</i> -Pr	0.14(0.04)	2.2
6d	<i>n</i> -butyl	0.19(0.04)	2.1
6e	<i>n</i> -octyl	0.55(0.4)	1.7
6f	<i>i</i> -Pr	0.18(0.1)	1.8
6g	<i>sec</i> -Bu	0.097(0.04)	2.0
6h	<i>tert</i> -Bu	0.65	2.1
6j	cyclohexyl	2.71	1.9
6k	cyclopentyl	0.47	1.9
6l	2-(1-methylpiperidinyl)	0.14(0.1)	1.9
6m	2-THP	0.48(0.06)	2.1

(chloro), methyl, and methoxy substituents was meta > ortho > para isomers (Table 2). In general, meta-substituted benzyloxy analogues featured better activity. Both electron-withdrawing and electron-donating meta-substituents groups (e.g., Cl, OMe, and Me) were well tolerated. The corresponding para isomers showed lower activity (e.g., **5b** vs **5c**, **2e** vs **5f**, and **5k** vs **5l**). Notably, trifluoromethyl substituents enhanced activity compared with the corresponding methyl isomer, suggesting the lipophilic nature of the binding pocket. Considering that all monofluoro isomers (2-, 3-, and 4-) had essentially identical activity, a number of difluoro analogues were synthesized and evaluated in the promoter assay. The 3,5-difluoro analogue **5p** was 8 and 14 times more potent than the 2,6-difluoro analogue **5t** and 2,4-difluoro **5s**, respectively. Compared to the substituted phenyl-CH₂ analogues, heterocyclic-CH₂ ethers (thiophene **5w**, furane **5x**, and isoxazole **5y**) generally had poor activity, 3-pyridyl analogue **5v** being an exception. The fused 3-pyridyl system, **5z**, displayed a 10-fold loss in activity. Several C5-OCH₂Ar/heterocyclic series provided potent analogues (EC₅₀ < 100 nM); however, the majority of these (with the exception of **5g** and **5v**) did not afford more than 2-fold induction of the SMN2 promoter above background.

With several potent analogues derived from the 5-benzyloxy series in hand, we synthesized 24 analogues varying the substitution pattern at the 6, 7, and 8 positions of the quinazoline core. However, all of these analogues were inactive in the promoter assay. In addition to the -O-Ar/heterocycle derived analogues, -S(O)_n, *n* = 0–2 (as mentioned above) and aza-linked C5 analogues (data not shown) were also prepared. These analogues were significantly less active than the respective C5 benzyloxy analogues discussed above.

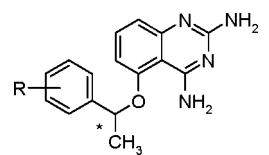
Nonaryl Ether Derivatives. 5-Ethoxyquinazoline **6b** was as active as reported by Jarecki et al.³ In follow-up SAR studies, a number of linear and branched alkoxy (C5-O-R) analogues were prepared. Substitution with linear alkyl radicals (**6a–d**) did not improve activity. Cycloalkyl and heterocyclic substituents (**6j–m**) also afforded disappointing results. On the other hand, branched alkyl derived ethers improved biological activity; e.g., (racemic) *sec*-Bu **6g** had EC₅₀ of ~100 nM (Table 3).

α -Alkyls as Conformationally Constrained Analogues. On the basis of the analysis of benzylic ethers and branched-alkyl

Table 4. Activity of C5-O-CH(R)-Phenyl Analogues in the SMN2 Promoter Assay


compd	SMN promoter EC ₅₀ (SD), μ M	R1	R2	chirality ^a
5b	0.078(0.03)	H	3-Cl	
7a	0.021(0.01)	Me	3-Cl	<i>RS</i>
5c	0.18(0.1)	H	4-Cl	
7b	0.080(0.06)	Me	4-Cl	<i>RS</i>
7c	0.17	Et	4-Cl	<i>RS</i>
7d	7.76	<i>tert</i> -Bu	4-Cl	<i>RS</i>

^a Compounds are racemates.

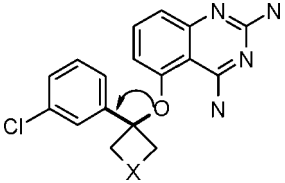
Table 5. Activity of Racemic C5-O-CH(CH₃)-Phenyl Analogues in the SMN2 Promoter Assay


compd	SMN promoter EC ₅₀ (SD), μ M	R	chirality ^a
7a	0.021 (0.01)	3-Cl	<i>RS</i>
7b	0.080 (0.06)	4-Cl	<i>RS</i>
7e	0.047 (0.03)	3-CF ₃	<i>RS</i>
7f	0.055 (0.04)	3-F	<i>RS</i>
7g	0.035 (0.04)	3,5-F ₂	<i>RS</i>
7j	0.018 (0.01)	4-F	<i>RS</i>
7k	0.050 (0.07)	4-CF ₃	<i>RS</i>
7m	0.32 (0.5)	3,4-Cl ₂	<i>RS</i>
7n	0.05 (0.04)	3-F	<i>RS</i>
7p	1.01 (0.3)	2-CF ₃	<i>RS</i>
7q	0.29 (0.2)	2-Cl	<i>RS</i>
7r	1.13	3,4-(OCH ₂ O)	<i>RS</i>
7s	0.44 (0.4)	2-naphth	<i>S</i>
7t	2.39	1-naphth	<i>S</i>

^a With the exception of **7s** and **7t**, which have (*S*)-chirality, all compounds are racemates.

ethers, it was postulated that the conformational constraints imposed by the α -substituent on the benzylic carbon might allow preorganization of the C5 substituents. This may enhance binding and show improved activity in the promoter assay. Following this hypothesis, we prepared a series of phenyl substituted α -methylbenzyl ether analogues. SAR data (Table 4) showed that an α -methyl substituent indeed improved potency (for example, **5b** vs **7a** and **5c** vs **7b**). Larger alkyl substituents were not tolerated. Both α -ethyl (**7c**) and α -*tert*-butyl (**7d**) substitution resulted in a significant drop in promoter activity. For example, the *tert*-butyl analogue was ~100-fold less active than the methyl analogue **7b**.

Encouraged by our initial results for chlorobenzyl analogues (Table 4), we prepared a number of additional α -methyl substituted molecules. As shown in Table 5, a number of 3- and 4-substituted phenyl compounds also showed good activity. Analogues **7p** and **7q** bearing ortho substituents displayed loss in activity. Analogues modified with bicyclic aromatics **7r**, **7s**, and **7t** allowed for the exploration of conformational space. Similar to the ortho substituents, 1-naphthyl analogue **7t** led to the greatest loss in activity compared to the 2-naphthyl analogue **7s**. Overall, a number of 3- and 4-substituted (racemic) α -methyl benzyl ethers provided SMN2 activators (as indicated by the promoter assay) with EC₅₀ in the 10–100 nM range (Table 5).

Table 6. Activity of α,α -Disubstituted Benzyl Ether Analogues in the *SMN2* Promoter Assay


compd	$-\text{CH}_2-\text{X}-\text{CH}_2-$	<i>SMN2</i> promoter EC ₅₀ (SD), μM	O–C–C(aryl) angle, deg ^a
5b	(reference)	0.078(0.03)	109.2
8a	dimethyl [X = absent]	2.33	103.7
8b	Cy-hexyl [X = (CH ₂) ₃]	1.71	101.5
8c	Cy-propyl [X = bond]	0.29(0.12)	121.5

^a Values derived from MMFF94 (SYBYL6.9) optimized geometries.

α,α -Disubstituted Analogues. Prior to embarking on enantioselective synthesis of individual α -methyl enantiomers, it was decided to evaluate the achiral α,α -disubstituted benzyl ether analogues. The *gem*-dimethyl analogue **8a** featuring an additional C-methyl group to **6b** resulted in about 100-fold loss in activity. Several cycloalkyl analogues with varying O–C–C(aryl) angle compared to the starting benzyl ether **5b** were synthesized (**8b**, **8c**). The cyclopropyl moiety was expected to have the least impact on the optimal topology of the appended 3-chlorophenyl group. The respective analogue **8c** possessing the largest angle (Table 7) was only 3-fold less active, while the cyclohexyl analogue **8b** was \sim 20-fold less active compared to benzyl ether **5b**. Analogues **8a** and **8b** with similar values for the O–C–C(aryl) angle had similar activity. Unfortunately, none of the achiral analogues derived from α,α -substitution provided improved *SMN2* promoter activity (Table 6).

Chiral α -Methyl Analogues. Because α -methyl was the optimal alkyl group, both enantiomers of **7a** were prepared and assayed to determine chiral preference for activity. Considering both the cell-based nature of the assay and about a 3- to 5-fold variation from experiment to experiment, EC₅₀ determinations for the racemate and the two enantiomers were carried out side by side in one experiment. The experiment (Table 7) showed that the (*S*)-enantiomer (*S*)-**7a** was 16 times more active than (*R*)-enantiomer (*R*)-**7a**. This (*S*)- vs (*R*)-enantiomeric preference was confirmed for the phenyl series (*S*)-**7u** vs (*R*)-**7u** as well.

Bioactive Orientation of the C5 Substituent. As mentioned above, increase in bulk for the α -alkyl substituent reduced activity. However, loss in activity going from a methyl to an ethyl substituent could be rationalized in terms of (a) a straightforward steric demand or (b) an unfavorable electronic environment of the terminal CH₃ group for the allowed orientation [A], of the $-\text{CH}_2-\text{CH}_3$, as depicted in Scheme 7. This analysis further suggested synthesis of the conformationally constrained ethyl analogue **C**. Because meta substituents provided greater activity, the corresponding isomeric cyclized analogues **D1** and **D2** were considered (Scheme 8).

Between the two possible chloroindanol derived ether analogues (Scheme 9), only the 6-chloroindanol derived analogue **6a** was active. The 4-chloroindanol derivative **6b** was inactive in the promoter assay. Incidentally, both the constrained analogue **6a** and the benzyl ether **2b** were equipotent.

Systematic conformational searches³⁸ with the 3-chlorophenyl **1c**, 3-chlorobenzyl **5b**, 3-chloro-(*S*)- α -methylphenyl (*S*)-**7a**, 6-chloroindanyl **9a**, and 4-chloroindanyl **9b** analogues were carried out with 10° increments using SYBYL. For each conformation, the vector tethering the oxygen atom to the para

carbon of the phenyl group was recorded (Figure 3). Vectors corresponding to conformations within 3 kcal/mol of the lowest energy conformation for each compound were plotted. Figure 4 shows that regions of vectors shared by more active benzyl ether analogues **5b** [magenta] and **7a** [blue] differ significantly from the phenyl ether analogue **1c** [cyan]. For clarity, vectors for the two indanol-derived products are shown in Figure 4b. On the basis of our data, active **9a** and inactive **9b** compounds access distinctly different conformational space. The region highlighted with the yellow oval (Figure 4c) represents the conformational space that is shared by all three active analogues **5b**, **7a**, and **9a**. For the inactive indane analogue **9b**, this conformational space is not accessible. Thus, **7a** represents the potential “bioactive” orientation of C5 substituents. This information was further used for the generation of a pharmacophore model of bioactivity.

Overcoming DHFR Inhibition as an Off-Target Activity. Selected quinazolines with *SMN2* promoter EC₅₀ < 100 nM were profiled across a panel of cellular toxicity assays. Specifically, we monitored proliferation, oxidative stress, mitochondrial function (as assessed by MTT metabolism), and energy metabolism (as assessed by measuring cellular ATP levels) (see Table 8). Data for compounds **5b**, **5c**, and **7a** indicated that MTT metabolism and ATP depletion were the most sensitive indicators of cellular toxicity.

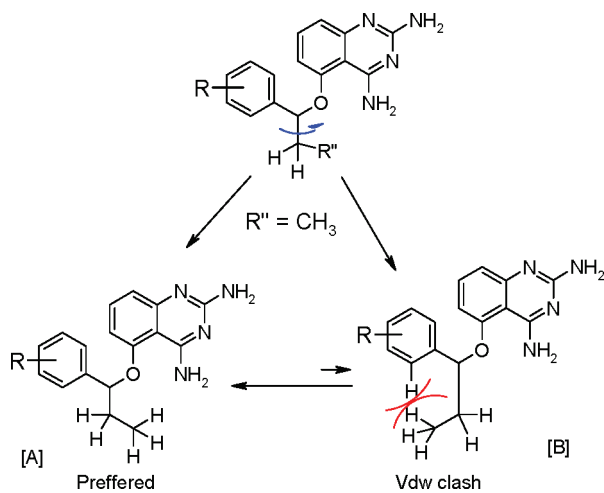
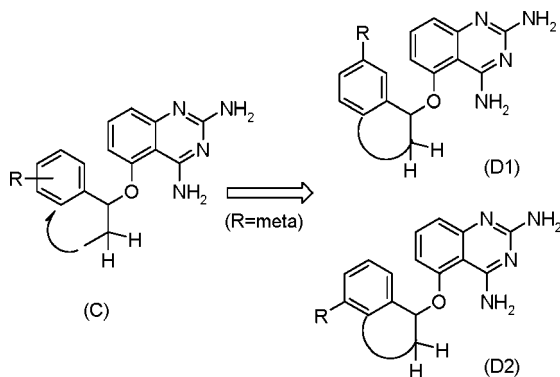
This led to the hypothesis that **5b**, **5c**, and **7a** either inhibit synthesis of ATP or accelerate hydrolysis of ATP resulting in cellular toxicity. Because the quinazoline core has been used to derive potent dihydrofolate reductase inhibitors (DHFR), e.g., methotrexate (MTX), and the folate pathway is involved in the synthesis of nucleoside triphosphates,⁴¹ it seemed possible that the cellular toxicity of the C5-quinazolines might be linked to DHFR inhibition. This was indeed the case as shown in Table 9, as potent DHFR inhibitors also potentially depleted cellular ATP.

At this juncture, it was important to determine whether (a) DHFR inhibition was a plausible mechanism for *SMN2* gene induction and, thus, if DHFR inhibition was linked to activity in the promoter assay or (b) if DHFR inhibition was simply an undesirable off-target activity. Methotrexate (MTX), a potent inhibitor of human DHFR (IC₅₀ = 1 nM), did not affect *SMN2* promoter activity at up to 30 μM , indicating that DHFR inhibition was an off-target activity.

High-resolution crystallographic data for inhibitor bound human DHFR are available in the public domain (Brookhaven PDB), facilitating structure-guided optimization of the C5-quinazolines in order to reduce or eliminate DHFR binding. As shown in Figure 5, target-bound TMQ-DHFR [TMQ = trimetrexate] crystal data clearly showed H-bond interactions of the 2- and 4-amino groups of the quinazoline core with key active site residues: Glu30, and Ile7 and Val115 of human DHFR.⁴² Approximately 40 analogues representing functionalization of the 2/4 amino groups had been prepared earlier in our program. Unfortunately, any modification or deletion of the C2- and/or C4-amino (NH₂) groups of the quinazoline analogues resulted in loss of promoter activity (data not shown). Thus, isosteric modifications of these amine functionalities did not represent a viable option to overcome DHFR inhibition. Considering that modification at the C5 position of the 2,4-diaminoquinazoline core allowed retention of promoter activity, our initial approach was directed toward modification of C5 substituents (juxtaposed to the C4-NH₂ group). We reasoned that these changes would perturb and/or disfavor the observed H-bonding interaction of the N⁴ amine hydrogens with human DHFR residues, e.g., at

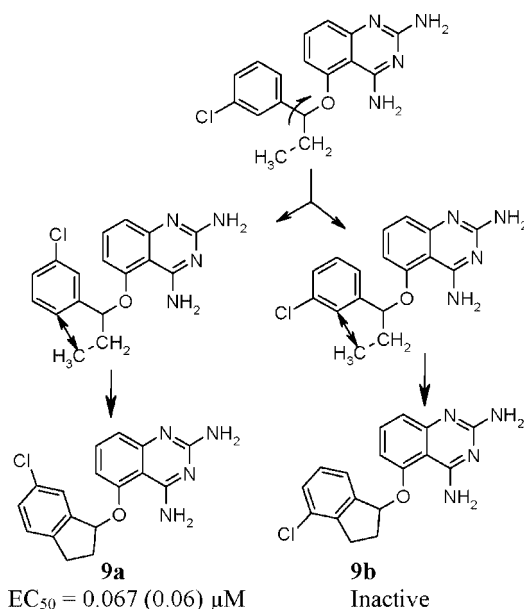
Table 7. SMN2 Promoter Assay Results for Chiral α -Methyl Benzyl Ether Analogues

compd (see above left)	chirality	EC ₅₀ (SD), μ M	compd (see above right)	chirality	EC ₅₀ (SD), μ M
7a	<i>RS</i>	0.021 (0.01)	7u	<i>RS</i>	0.24
(<i>R</i>)- 7a	<i>R</i>	0.032	(<i>R</i>)- 7u	<i>R</i>	0.22 (0.08)
(<i>S</i>)- 7a	<i>S</i>	0.002	(<i>S</i>)- 7u	<i>S</i>	0.06 (0.05)

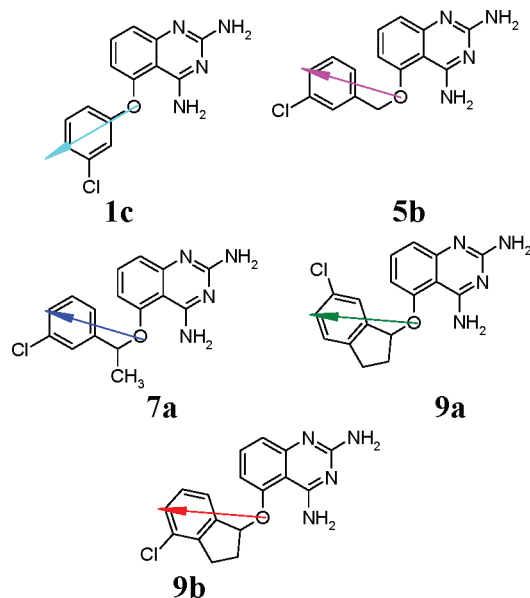
Scheme 7**Scheme 8**

least Val115 or preferably both Ile7 and Val115 (proposals A, B, Scheme 10). Proposal A involved incorporation of a suitably placed hydrogen bond acceptor, whereas proposal B incorporated an H-bond donor/acceptor.⁴³

SAR for Reverse Benzyl Ethers. Initially, we planned to prepare analogues with the oxygen (one or more) atom(s) removed from the quinazoline core. As a result, several analogues with the general structure referred to as “reverse benzyl series” (Scheme 10) were prepared and tested in both SMN2 promoter and DHFR assays. In these series, halogen substituents (Cl and F) provided better activity than methyl and methoxy, similar to the SAR data discussed above. Among chloro isomers, the activity decreased in the following order: meta > para > ortho. The respective para isomers were ranked as follows: F > Cl > CH₃ >> OCH₃ (Table 10). Among disubstituted phenyl analogues, 2,4-difluoro analogue **10b** was more potent. Data in Table 11 provide a comparison of two

Scheme 9

isomeric benzyl ether series: **5** vs **10**. It shows that not only did the isomeric benzyl series **10** provide analogues with good activity, these analogues also showed higher fold induction of the SMN2 promoter. More importantly, these analogues displayed 10- to 20-fold improvement in selectivity over DHFR inhibition⁴⁴ compared with the benzyl ether analogues **5**.

**Figure 3.** Compounds used for systematic conformational search with vectors plotted in Figure 4 highlighted.

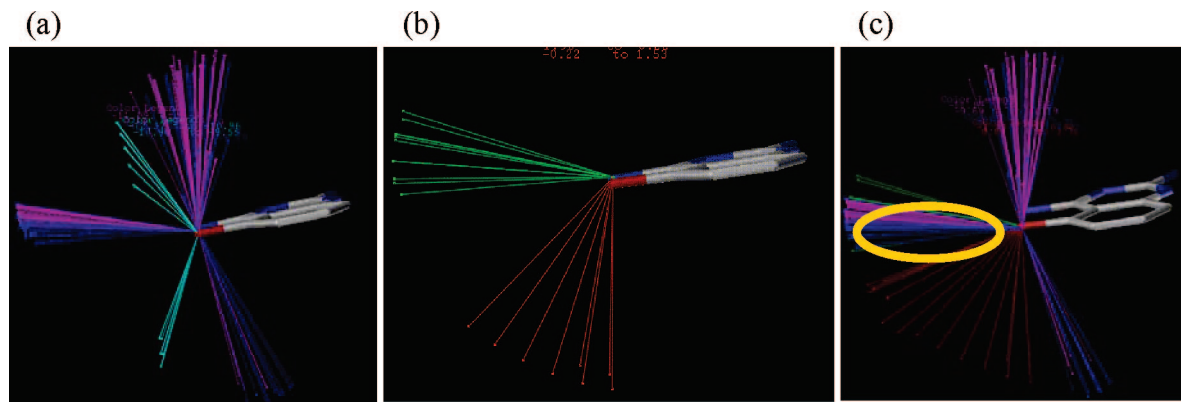


Figure 4. Vector maps corresponding to 3-chlorophenyl **1c** [cyan], 3-chlorobenzyl **5b** [magenta], 3-chloro- α -methylphenyl **7a** [blue], 6-chloroindane **9a** [green], and 4-chloroindane **9b** [red]: (a) vectors corresponding to **1c**, **5b**, and **7a**; (b) vectors corresponding to **9a** and **9b**; (c) vectors corresponding to **5b**, **7a**, **9a**, and **9b**. Vector maps were generated using SYBYL 6.0/7.0.³⁹ See Experimental Section for details.

Table 8. Cellular Toxicity Screen Using Rat Hepatoma Cell Line^{40,a}

compd	cell no. TC ₅₀ , μ M	GST TC ₅₀ , μ M	MTTTC ₅₀ , μ M	ATP TC ₅₀ , μ M
5c	32	71	36	0.1
5b	5	29	8	0.3
7a	1	55	4	1

^a GST, α -glutathione *S*-transferase; MTT, 3-[4,5-dimethylthiazol-2-yl]-2,5-diphenyltetrazolium bromide; ATP, adenosine triphosphate; TC₅₀, concentration that produced a half-maximal response, cellular toxicity.

Table 9. *SMN2* Promoter Induction vs DHFR Inhibition

compd	DHFR IC ₅₀ , nM (average <i>n</i> = 2)	<i>SMN2</i> promoter induction (EC ₅₀ , nM)
5b	98	78
7a	34	21
(<i>S</i>)- 7a	25	2
methotrexate	1	inactive (no induction up to 30 μ M)

A number of molecules featuring desirable *SMN2* promoter activity and \sim 100-fold range of DHFR inhibition were evaluated in the cellular toxicity panel. A scatter plot of these data is shown in Figure 6. The good correlation ($r^2 = 0.87$) for ATP depletion TC₅₀ vs DHFR IC₅₀ further supported the hypothesis that cellular toxicity was linked to DHFR inhibition. Thus, our structure-

guided approach provided an efficient means to overcome DHFR off-target activity for this series of quinazolines.

Piperidine Series. To improve further the separation between *SMN2* promoter induction and potential for DHFR inhibition, a number of C5 substituents were investigated that would exceed spatial limitations imposed by the DHFR active site (Figure 7). Piperidine-derived analogues **11–13** are examples of these series. Both synthetic flexibility and the achiral nature of these agents allowed for rapid SAR studies of promoter activity and DHFR inhibition (Scheme 6). A diverse range of substituents were explored to evaluate contribution of size and shape, H-bond donor/acceptor features, and the ionic nature of the substituents. In addition, the tether "X" was varied (e.g., X = CH₂, CO, and SO₂). Over 125 analogues were prepared to study SAR within these series. Table 12 shows a selected set of N-substituted piperidine analogues. In general, this pharmacophore provided a number of potent analogues with good to excellent promoter activity and sound maximum fold induction. The nature of the "X" group also influenced the activity. Tertiary amine analogues **11** displayed the best activity compared to the corresponding amide **12**. These in turn were better than the corresponding sulfonamides **13**. A wide range of functional groups for the tertiary amine analogues were tolerated, several analogues showing EC₅₀ < 100 nM. Although the preference for linker "X" was CH₂ > CO \gg SO₂, there were some notable exceptions to this trend. This included the 3,4-difluoro set, where the tertiary amine analogue **11k** had poor promoter activity compared with the corresponding amide **12k** and sulfonamide **13k**. Steric bulk explored with the **11e/12e/13e** and **11f/12f/13f** sets, where the "R-Ph" substituent was replaced with 1- and 2-naphthyl derivatives, identified the 2-naphthyl pharmacophore as the worst, irrespective of the nature of the linking group "X". A number of difluoro derivatives, except 3,4-difluoro, displayed similar activity. The 2-fluorophenyl substituent yielded the best EC₅₀. Although amide derivatives in general had lower EC₅₀ than the respective tertiary amines, they afforded higher maximum fold induction. It was gratifying to see that the majority of piperidine analogues showed weak DHFR inhibition (IC₅₀ \gg 125 μ M) except for the benzylpiperidine analogue **11b**.

A significant portion of the derivatized piperidine analogues showed good-to-excellent activity in the promoter assay, several with maximum fold induction in the range of 2–2.5. The vast majority of these compounds also showed good metabolic stability. Selected compounds evaluated for human cytochrome P450 (hCYP) inhibition also posed no concern. In order to identify compounds with high brain exposure and to further

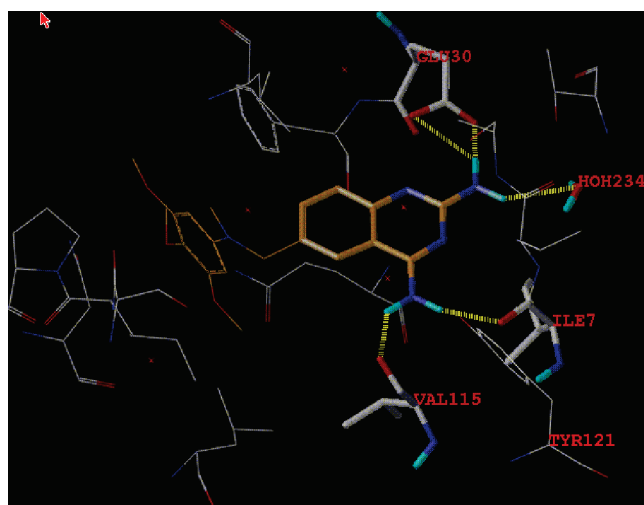


Figure 5. Human DHFR-bound ligand (1s3u.pdb). H-bonds of the two amino groups of the quinazoline core and the DHFR amino acid residues are highlighted.

Scheme 10. Proposals To Disrupt Atypical Quinazoline–DHFR H-Bond Interactions

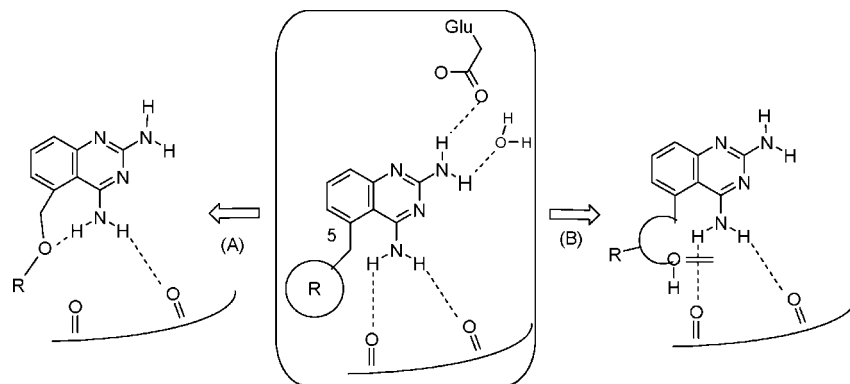
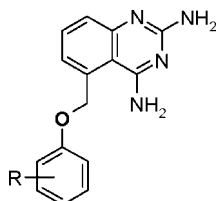


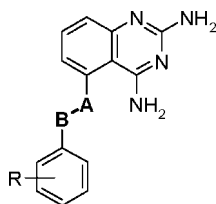
Table 10. Activity of C5-CH₂O-Ar (Reverse Benzyl) Analogues in the SMN2 Promoter Assay



compd	Phenylsubstituents	EC ₅₀ (SD), μM	MFI ^a	DHFR IC ₅₀ , μM
10a	3-Chloro	0.042 (0.03)	2.0	8.4
10b	2-Chloro	1.16 (1.0)	2.2	
10c	2-Iodo	0.39 (0.2)	1.9	
10d	2-Fluoro	0.019 (0.01)	2.1	39.0
10e	4-Methyl	0.41 (0.4)	2.2	
10f	4-Chloro	0.19 (0.04)	2.0	
10g	4-Fluoro	0.35 (0.3)	2.2	
10h	4-Methoxy	1.40 (0.2)	2.1	
10i	2,4-Difluoro	0.042 (0.01)	2.2	5.1

^a MFI = Maximum Fold Induction.

Table 11. Comparison of Two Isomeric Benzyl Ether Series



R	compd	A-B = -CH ₂ -O-		A-B = -O-CH ₂ -	
		EC ₅₀ , μM (MaxFoldInd)	DHFR IC ₅₀ , μM	EC ₅₀ , μM (MaxFoldInd)	DHFR IC ₅₀ , μM
2-F	10d	0.019(2.1)	39.0	5g	0.053(1.8)
2,4-F2	10i	0.042(2.2)	10.7	5s	0.12(1.8)
3-Cl	10a	0.042(2.0)	8.4	5b	0.078(1.8)

prioritize these for in vivo experiments, active compounds were dosed in mice at 2 mg/kg (iv). Concentrations of parent compound were measured in plasma and brain samples using LC/MS/MS at 15 min and 2 h postdose with $n = 4$ mice per time point. Data for these two time points helped sort compounds based on relative apparent $t_{1/2}$ and relative trend for brain/plasma exposure. A summary of these data for selected compounds is shown in Table 13. Across three piperidine series, good blood–brain barrier permeability was achieved if the polar surface area (PSA) was below 90 Å².

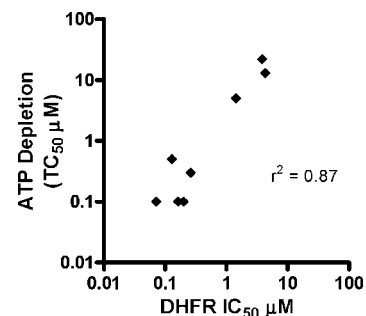


Figure 6. Correlation of TC₅₀ for ATP depletion using rat hepatoma (H4IIE) cell line versus IC₅₀ for DHFR inhibition for C5-functionalized 2,4-diaminoquinazoline analogues. All of the analogues shown here also have good activity in the SMN2 promoter assay.

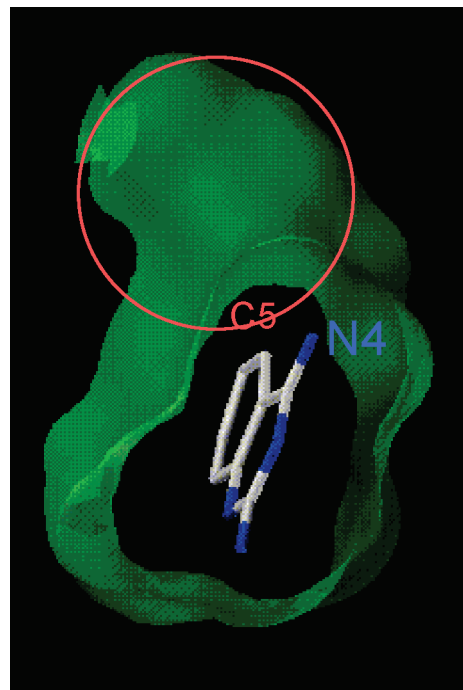
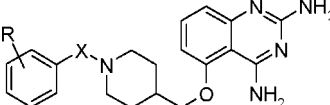


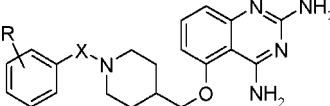
Figure 7. Size and shape of the pocket for a potential substituent projected from C5-position of quinazoline is highlighted by an orange circle. This orientation of quinazoline shown is identical to that of 2,4-diamino pteridine (bicyclic core structure) of MTX and the A-ring containing 2,4-diamino portion overlaps with the tetrahydrofolate-derived DHFR bound ligand in 1s3u.pdb. See Experimental Section for details.

Subsequently, full PK analysis for **11a** was carried out following iv and oral dosing. The resulting data reconfirmed that **11a** possessed a long brain half-life ($t_{1/2} \approx 19$ h) (Table 14)

Table 12. Activity of N-Substituted Piperidines Series in the *SMN2* Promoter Assay


The chemical structure shows a piperidine ring connected via an X group to a phenyl ring with an R substituent. The piperidine ring is also connected via a methylene group to an oxygen atom, which is part of a quinazolinone ring system with two amino groups (NH₂).

R	X = CH ₂			X = CO			X = SO ₂		
	compd	EC ₅₀ (SD), nM	MFI ^a	compd	EC ₅₀ (SD), nM	MFI ^a	compd	EC ₅₀ (SD), nM	MFI ^a
2-F	11a	4 (1)	2.4	12a	74	2.5	13a	29	2.1
3-Cl	11b	54 (10)	2.2	12b	60 (10)	2.3	13b	172 (40)	1.9
2-Cl	11c	38 (10)	2	12c	49 (10)	2.4	13c	897	2.1
4-Cl	11d	47 (30)	1.8	12d	81 (30)	2.4	13d	603	2
1-naphth	11e	43 (30)	2	12e	35 (10)	2.5	13e	350	1.9
2-naphth	11f	148 (70)	1.7	12f	151 (90)	2.4	13f	464	2
2-Me	11g	18 (10)	1.9	12g	160 (40)	2.5	13g	545	2
3-Me	11h	22 (10)	1.9	12h	110 (70)	2.2	13h	221	1.8
4-Me	11i	24 (10)	1.9	12i	133 (30)	2.6	13i	551	1.9
2,4-F ₂	11j	18 (10)	1.9	12j	89 (30)	2.4	13j	82 (40)	2
3,4-F ₂	11k	322 (80)	2	12k	104 (10)	2.4	13k	133 (40)	2.1
2,3-F ₂	11m	38 (10)	2.2	12m	67 (10)	2.5			

^a MFI = maximum fold induction.**Table 13.** Plasma and Brain Levels at 15 min and 2 h and Key in Vitro Data for Selected Piperidine-Derived Analogues^a


compd	X	R	SMN2 promoter		plasma levels, ng/mL		brain levels, ng/g	
			EC ₅₀ , μM	DHFR IC ₅₀ , μM	15 min	120 min	15 min	120 min
11a	CH ₂	2-F	0.004	> 125	38	21	1423	1133
12c	CO	2-Cl	0.014	> 125	240	20	26	9
12b	CO	3-Cl	0.060	> 125	225	17	23	10
11b	CH ₂	3-Cl	0.054	55.2	462	610	1150	1518
13a	SO ₂	2-F	0.029	> 125	279	25	305	106

^a All compounds were dosed at 2 mg/kg in 30% solutol.**Table 14.** Pharmacokinetic Parameters for Piperidine Analog **11a** Following iv and po Dosing to Mice^a

route (iv)	parameters	units	values	SD	route (po)	parameters	units	values	SD	
iv plasma	<i>t</i> _{1/2}	h	NA		iv plasma	IC _{max}	ng/mL	110	28.7	
	AUC _{last}	h•ng/mL	2406	9.95		<i>t</i> _{1/2}	h	NA		
	Cl _{pred}	(mL/h)/kg	83.8	74.0		AUC _{last}	h•ng/mL	2673	45.6	
	V _{ss,pred}	mL/kg	38103	2584		AUC _{INF}	h•ng/mL	10893	3443	
iv brain	<i>t</i> _{1/2}	h	18.96	1.32	iv brain	C _{max}	ng/g	765.00	129	
	AUC _{last}	hr•ng/g	15724	1118		<i>t</i> _{1/2}	h	18.80	0.95	
	Cl _{pred}	(g/h)/kg	110	8.6		AUC _{last}	h•ng/g	15485	931	
	V _{ss,pred}	g/kg	2437	230		AUC _{INF}	h•ng/g	18910	1041	
	MRT _{INF}	h	22.83	0.995		MRT _{INF}	h	27.30	1.22	

^a Compound was dosed in 30% solutol at 2 mg/kg iv and in HPMC-Tween-80 at 10 mg/kg, orally.

with low plasma and brain clearance. This compound showed very good brain exposure and overall coverage measured as brain-to-plasma ratio based on C_{max} or AUC, as both of these ratios were about 5- to 6-fold higher in brain vs plasma. Compound **11a** also had very low potential for drug–drug interaction because it did not inhibit any of the major human cytochrome P450 enzymes (hCYP). Specifically, **11a** inhibited hCYP2D6 with an IC₅₀ of 9.38 μM whereas inhibition of all other enzymes tested (CYP1A2, CYP2C9, CYP2C19, and CYP3A4) was <50% at 10 μM. Compound **11a** displayed attractive physicochemical properties, with 41.5 mg/mL solubility in water as a dihydrochloride salt.

Next, the piperidine analogue **11a** was evaluated as a modulator of (a) the endogenous *SMN* promoter in the mouse NSC-34 cell line and (b) human Smn protein levels in SMA type I patient fibroblast cell lines. To test effects on the mouse *SMN* promoter, **11a** was incubated with NSC-34 cells for 18 h

using the conditions that were described for the promoter assay. Cells from multiple wells were pooled, and RNA was isolated for sequential cDNA generation and TaqMan analysis (see Experimental Section for details). Compound **11a** increased mouse *SMN* mRNA about 2-fold in NSC-34 cells (Figure 8), an effect similar in magnitude to the induction of the engineered human *SMN2* reporter gene. Although the mechanism of promoter induction by **11a** or the other quinazoline analogues is unknown, this demonstrates that *SMN* promoter induction is independent of chromosomal location or the local state of chromatin activation. Trichostatin A, a histone deacetylase inhibitor that potently induces *SMN2* gene activity, was used as a positive control in this experiment. Selected C5-substituted quinazolines did not inhibit histone deacetylase (data not shown) as shown previously by Jarecki et al.³³

To examine the effect of these quinazoline derivatives on human *SMN* expression, we treated a fibroblast cell line from

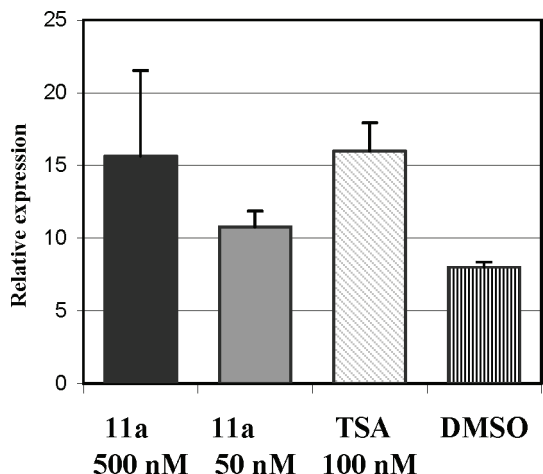


Figure 8. Effect of compound **11a** and its comparison with TSA on mouse SMN mRNA expression in the murine NSC-34 cell line under serum-free media conditions.

a type I SMA patient (line 3813) with different doses of **5b**, **11a**, or **11b**. In the 3813 cell line, *SMN1* has been deleted from both chromosomes and *SMN2* is present at low copy number. For comparison, line 3814 is a fibroblast line derived from the carrier parent and represents 50% normal SMN levels due to the deletion of the *SMN1* gene on only one of the two parental chromosomes. All three compounds increased amounts of SMN protein in a dose-dependent manner (Figure 9C).

SMN localizes to discrete granules in the nucleus called gems. The number of nuclei with gems and the number of gems per cell is reduced in type 1 SMA cells.¹¹ Compounds such as butyrate, 4-phenylbutyrate, valproate, and alcurubicin increase the number of gems in SMA fibroblasts.^{28–33} In the experiment, SMA patient fibroblasts were treated with increasing doses of **5b**, **11a**, or **11b** (10–1000 nM) for 5 days and the number of nuclei with gems as well as the number of gems per 100 nuclei were determined. All three compounds increased both the number of cells with gems (Figure 9A) and the number of gems (Figure 9A) in a dose-dependent manner. For instance, 100 nM **5b** increased the number of gems by ~2.9-fold (19.7 ± 2.6 for

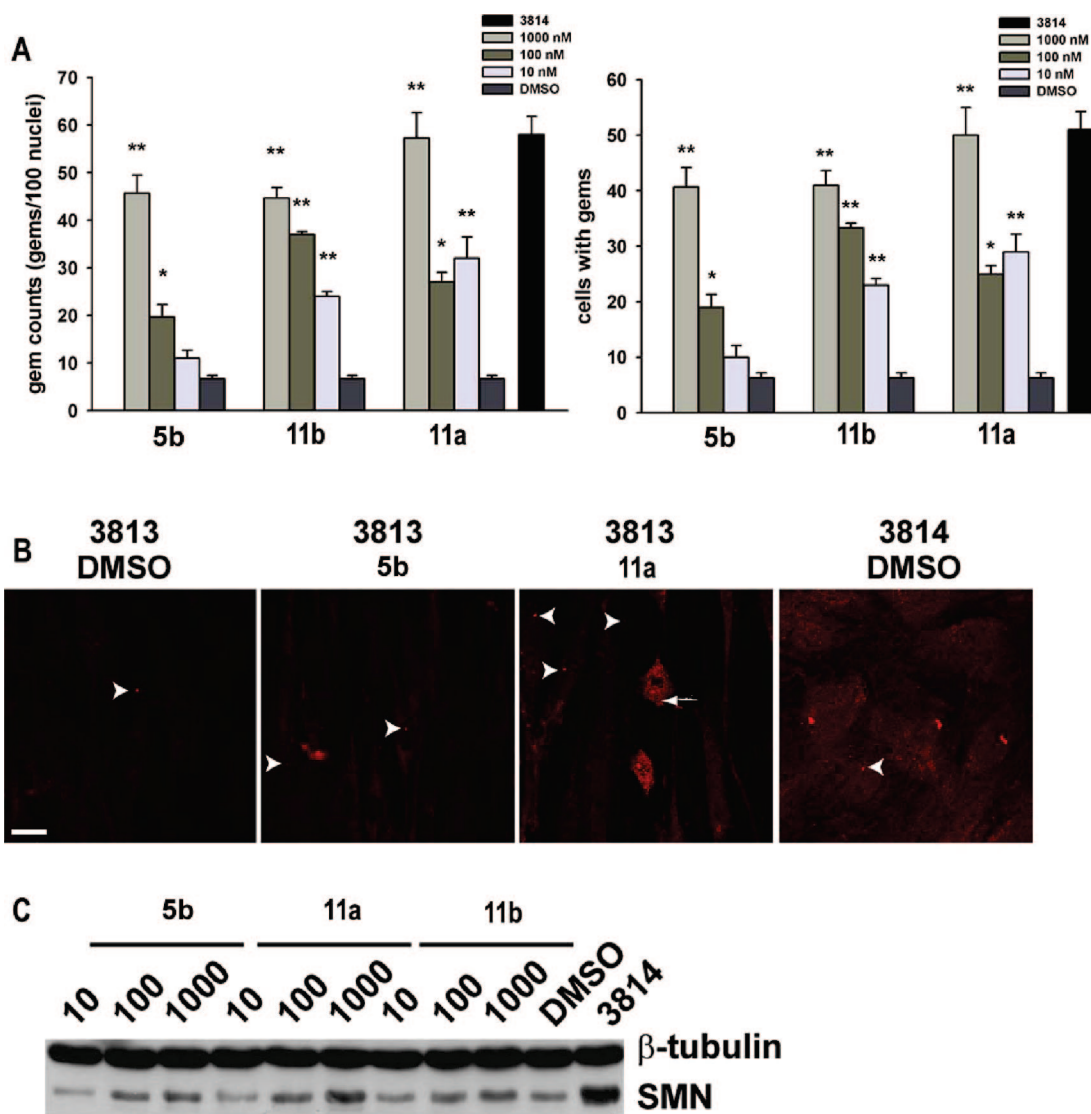


Figure 9. Effect of quinazoline derivatives on SMN expression in SMA patient fibroblasts. (A) Change in gem number per cell and number of gems per 100 nuclei after treatment with the drugs **5b**, **11a**, and **11b** at the concentration indicated. * indicates $p < 0.05$. ** indicates $p < 0.005$. The cell 3814 is derived from the carrier parent and represents the levels trying to be obtained. (B) Examples of 3813 cell after treatment stained with SMA antibody MANSMA2 (red). Arrow heads indicate gems, and arrow indicates cytoplasmic staining. (C) Western blot of SMN levels after treatment with drug compounds as indicated. Notice dose–response to drugs.

5b versus 6.7 ± 0.7 for DMSO; $n = 3$ per group; $p = 0.04$) while the same doses of **11a** and **11b** elevated the number of gems by ~ 5.5 -fold (37.0 ± 0.6 , $n = 3$, $p < 0.001$) and ~ 4.0 -fold (27.0 ± 2.1 , $n = 3$, $p = 0.026$), respectively. Interestingly, compounds **11a** and **11b** showed an increase in cytosolic staining whereas **5b** did not appreciably affect SMN staining in the cytosol (Figure 9B).

These studies confirmed that the piperidine **11a** up-regulated the mouse SMN promoter in NSC-34 cells, a mouse motor neuron derived cell line. It also up-regulated the endogenous human *SMN2* promoter in its normal chromosomal context. The compound increased full-length human Smn protein, as demonstrated by an increase in gems number in type I SMA patient fibroblasts. Gems were restored to a level similar to carriers. In vivo evaluation of compound **11a** in a transgenic mouse SMA disease model will be reported in due course.

Conclusion

Utilizing the uHTS hit reported by Jarecki et al.³³ as the starting point the uHTS hit reported by Jarecki et al.,³³ our ligand-based design strategy led to the identification of a series of C5 substituted 2,4-diaminoquinazolines (for example, **5b**) as inducers of the *SMN2* promoter. Introduction of α -methyl substituents provided conformationally constrained analogues with improved activity (lower EC_{50} and higher maximum fold induction) in the *SMN2* promoter assay compared with **5b**; however, in vitro assessment of cellular toxicity led to identification of DHFR inhibition as an off-target activity. A focused, structure-guided approach employing molecular modeling yielded achiral piperidine series **11–13** decoupled from the DHFR inhibition liability. Our best molecule **11a** showed a promising in vitro profile ($EC_{50} = 4$ nM, $EC_{90} = 70$ nM, MaxFoldInd = 2.4 in the NSC-34 cell assay). Furthermore, **11a** showed desirable pharmaceutical properties and excellent brain exposure ($C_{max} = 3$ μ M, following 10 mg/kg po dose and $t_{1/2} = 19$ h) following oral dosing in mice. This agent also up-regulated the mouse *SMN* promoter in a mouse motor neuron derived cell line, NSC-34. In addition, compound **11a** also up-regulated the human *SMN2* promoter in severe type I SMA patient fibroblasts and increased full-length human SMN protein as demonstrated by an increase in intranuclear gems, or Cajal bodies. The increase in the number of gems observed with the piperidine analogue **11a** was far superior to that observed for the initial uHTS hit **1b**. Gems were restored to the level of unaffected genetic carriers of the heterozygous *SMN1* gene deletion. We anticipate that our lead candidate **11a** will provide a tool for exploring therapeutic benefits of *SMN2* promoter induction in transgenic mouse models of SMA disease and ultimately in human clinical trials.

Experimental Section

Chemistry. General Methods. All reagents and anhydrous solvents were obtained from commercial sources and used without further purification unless otherwise noted. NMR spectra were recorded at either 400 or 500 MHz in the solvent indicated, TMS being an internal reference. Coupling constants (J) are given in Hz. Column chromatography was carried out in the solvents indicated with silica gel. HPLC purity of compounds was measured with a reversed-phase HPLC (Zorbax SB-C₁₈ column, 4.6 mm \times 150 mm, 5 μ m, 254 nm) with two diverse solvent systems. In system 1, compounds were eluted using a gradient elution 95/5 to 5/95 A/B over 20 min at a flow rate of 1.0 mL/min, where solvent A was aqueous 0.05% TFA and solvent B was acetonitrile (0.05% TFA). In system 2, compounds were eluted using a gradient of 95/5 to 5/95 A/C over 20 min at a flow rate of 1.0 mL/min, where

solvent A was aqueous 0.05% TFA and solvent C was methanol. Chiral HPLC was performed with a Chiralcel OD-H column eluted with a mixture of hexane and ethanol containing 0.1% trifluoroacetic acid. Chiral HPLC was performed with a Chiralcel OD-H column (250 mm \times 4.6 mm, 5 μ m, 254 nm) eluted with a mixture of hexane (containing 0.1% trifluoroacetic acid) and ethanol (7% ethanol isocratic elution over 45 min). Elemental analyses were carried out by Galbraith Laboratories, Inc. (Knoxville, TN) or Midwest Microlab, LLC (Indianapolis, IN). Mass spectra were obtained using either APCI or electrospray ionization.

General Procedure A: Preparation of 5-Aryloxy or 5-Substituted Aryloxymethyl 2,4-Diaminoquinazoline. Step 1: Preparation of 2-Fluoro-6-(aryloxy/alkoxy)benzotrile (4). A solution of substituted phenol or substituted benzyl alcohol (10 mmol, 1 equiv) was added to a cooled (0 $^{\circ}$ C) slurry of sodium hydride (washed w/hexanes) (0.407 g, 10 mmol, 1equiv) in DMF (7 mL) under nitrogen atmosphere. The reaction mixture was slowly warmed to room temperature and stirred for 1 h. The reaction mixture was then added to a cooled (0 $^{\circ}$ C) solution of 2,6-difluorobenzotrile **2** (7–10 mmol, 0.7–1.0 equiv) in DMF (5 mL) and stirred for 3–5 h at room temperature. The reaction mixture was poured on crushed ice–water, stirred, filtered, and washed with water. The resulting solid was filtered and dried in vacuo to afford 2-fluoro-6-(aryloxy/benzyloxy)benzotrile intermediate.

Step 2. Cyclization of 2-Fluoro-6(aryloxy/substituted benzyloxy)benzotrile (4) to 5-Ether Derivatives of 2,4-Diaminoquinazoline. Guanidine carbonate (180 mg, 1.0 mmol, 2 equiv) and 2-fluoro-6(aryloxy/substituted benzyloxy)benzotrile (0.5 mmol, 1 equiv) were heated at 140 $^{\circ}$ C in dimethylacetamide (2 mL) for 10 h and allowed to cool to room temperature overnight. The reaction mixture was further cooled in the refrigerator. The resulting solid was collected in vacuo and recrystallized from ethanol/water to provide the quinazoline derivative.

5-(2-Chlorophenyl)quinazoline-2,4-diamine (1e). 2-Chlorophenol (1.1 mL, 10 mmol) and sodium hydride (0.407 g, 10 mmol) was reacted with 2,6-difluorobenzotrile (1.39 g, 10 mmol) in DMF (5 mL) using procedure A, step 1, to afford 0.746 g of 2-fluoro-6-(2-chlorophenyl)benzotrile (22% yield). 2-Fluoro-6-(2-chlorophenyl)benzotrile (229.3 mg, 0.9 mmol) and guanidine carbonate (147.2 mg, 0.8 mmol) were reacted according to procedure A, step 2. The solid was recrystallized from ethanol/water, 1:1, and dried in vacuo to yield 119.7 mg of 5-(2-chlorophenyl)quinazoline-2,4-diamine (46% yield). HPLC $t_R = 8.6$ min (system 1), 11.8 min (system 2). 1H NMR (500 MHz, DMSO- d_6) δ 7.66 (dd, $J = 1.5, 8.5$ Hz, 1H), 7.44 (m, 1H), 7.32 (m, 3H), 7.19 (bs, 2H), 6.90 (dd, $J = 1.0, 8.5$ Hz, 1H), 6.09 (s, 2H), 6.01 (dd, $J = 0.5, 8.0$ Hz, 1H). MS m/z (ESI) 289 (M + H)⁺.

Compounds **1d** and **1f** were prepared analogous to the synthesis of **1e**.

5-(4-Fluorophenoxy)quinazoline-2,4-diamine (1d). Yield = 39%. HPLC $t_R = 8.5$ min (system 1), 11.6 min (system 2). 1H NMR (400 MHz, DMSO- d_6) δ 8.32 (s, 1H), 7.33–7.21 (br, m, 6H), 6.90 (d, $J = 8.4$ Hz, 1H), 6.15 (d, $J = 8.0$ Hz, 1H), 6.09 (br s, 2H). MS m/z (ESI) 271 (M + H)⁺.

5-(3-Chlorophenyl)quinazoline-2,4-diamine (1f). Yield = 46%. HPLC $t_R = 9.0$ min (system 1), 12.4 min (system 2). 1H NMR (500 MHz, DMSO- d_6) δ 7.46 (t, $J = 8.0$ Hz, 1H), 7.37 (t, $J = 8.0$ Hz, 1H), 7.28 (m, 2H), 7.09 (m, 1H), 7.04 (bs, 1H), 6.97 (dd, $J = 1.0, 8.0$ Hz, 1H), 6.31 (dd, $J = 1.0, 8.0$ Hz, 1H), 6.10 (s, 2H), 6.01 (m, 1H). MS m/z (ESI) 289 (M + H)⁺.

5-(2-Chlorobenzyl)quinazoline-2,4-diamine (5a). 2-Chlorobenzyl alcohol (1.54 g, 10.8 mmol), sodium hydride (60%, 432 mg, 10.8 mmol) in DMF (5 mL) were reacted with 2,6-difluorobenzotrile (1 g, 7.2 mmol) in DMF (20 mL) according to procedure A. Purification by recrystallization from cyclohexane yielded 1.69 g of 2-fluoro-6-(2-chlorobenzyl)benzotrile (85% yield). 2-Fluoro-6-(2-chlorobenzyl)benzotrile (131.1 mg, 0.5 mmol) and guanidine carbonate (110 mg, 0.6 mmol) were reacted according to procedure A. The solid was recrystallized from ethanol/water, 1:1, and dried in vacuo to yield 50 mg of 5-(2-chlorobenzyl)quinazoline-2,4-diamine (33% yield). 1H NMR (500 MHz,

DMSO- d_6) δ 7.63 (dd, $J = 7.5, 2.5$ Hz, 1H), 7.56 (dd, $J = 7.5, 1.5$ Hz, 1H), 7.40 (m, 3H), 7.17 (br d, 2H), 6.81(d, $J = 8.5$ Hz, 1H), 6.83 (d, $J = 8.0$ Hz, 1H), 6.01 (br s, 2H), 5.33 (s, 2H). ^{13}C NMR (500 MHz, DMSO- d_6) δ 161.7, 160.7, 133.5, 133.0, 132.3, 130.9, 130.4, 129.7, 127.6, 117.5, 101.8, 101.3, 67.7. MS m/z (ESI) 299 (M - H) $^+$. HPLC $t_R = 9.1$ min (system 1), 12.3 min (system 2).

Compounds **5b**–**y** were prepared similar to that described for **5a**.

5-(3-Chlorobenzoyloxy)quinazoline-2,4-diamine (5b). Yield = 37%. ^1H NMR (500 MHz, DMSO- d_6) δ 7.60 (s, 1H), 7.45 (m, 3H), 7.33 (t, $J = 8.0$ Hz, 1H), 7.23 (br d, 2H), 6.78 (d, $J = 8.5$ Hz, 1H), 6.58 (d, $J = 8.0$ Hz, 1H), 5.97 (br s, 2H), 5.29 (s, 2H). ^{13}C NMR (500 MHz, DMSO- d_6) δ 161.7, 160.7, 155.9, 155.2, 139.0, 133.2, 132.3, 130.6, 128.1, 127.8, 126.6, 117.3, 102.1, 101.4, 69.0. MS m/z (ESI) 299 (M - H) $^+$. FTIR 3515, 3397, 3345, 3120, 1652, 1615, 1596, 1575, 1552, 1500, 1479, 1435, 1407, 1371, 1356, 1254, 1178, 1130, 1081, 990, 863, 812, 784, 745, 686 cm^{-1} . Anal. ($\text{C}_{15}\text{H}_{13}\text{ClN}_4\text{O}$) C, H, N.

5-(4-Chlorobenzoyloxy)quinazoline-2,4-diamine (5c). Yield = 35%. ^1H NMR (500 MHz, DMSO- d_6) δ 7.48 (dd, $J = 9.0, 8.5$ Hz, 3H), 7.32 (t, $J = 8.0, 8.5$ Hz, 1H), 7.20 (bd, $J = 23.5$ Hz, 2H), 6.77 (d, $J = 8.0$ Hz, 1H), 6.58 (d, $J = 8.0$ Hz, 1H), 5.95 (s, 2H), 5.27 (s, 2H). MS m/z (ESI) 301 (M + H) $^+$. HPLC $t_R = 9.3$ min (system 1), 12.5 min (system 2).

5-(3-Methylbenzoyloxy)quinazoline-2,4-diamine (5e). Yield = 16%. ^1H NMR (500 MHz, DMSO- d_6) δ 7.32 (m, 4H), 7.19 (m, 3H), 6.77 (d, $J = 8.5$ Hz, 1H), 6.62 (d, $J = 8$ Hz, 1H), 5.94 (s, 2H), 5.21 (s, 2H), 2.34 (s, 3H). MS m/z (ESI) 281 (M + H) $^+$. HPLC $t_R = 9.2$ min (system 1), 12.4 min (system 2).

5-(4-Methylbenzoyloxy)quinazoline-2,4-diamine (5f). Yield = 39%. ^1H NMR (500 MHz, DMSO- d_6) δ 7.41 (d, $J = 7.5$ Hz, 2H), 7.35 (t, $J = 8$ Hz, 1H), 7.24 (d, $J = 8$ Hz, 2H), 7.6 (br d, $J = 28$ Hz, 2H), 6.77 (d, $J = 8.5$ Hz, 1H), 6.63 (d, $J = 8$ Hz, 1H), 5.92 (br s, 2 H), 5.20 (s, 2H), 2.32 (s, 3H). MS m/z 281 (M + H) $^+$. HPLC $t_R = 9.2$ min (system 1), 12.5 min (system 2).

5-(2-Fluorobenzoyloxy)quinazoline-2,4-diamine (5g). Yield = 22%. ^1H NMR (400 MHz, DMSO- d_6) δ 7.61 (m, 1H), 7.47 (m, 1H), 7.31 (m, 3H), 7.13 (br d, $J = 10.8$ Hz, 2H), 6.79(d, $J = 9.2$ Hz, 1H), 6.67 (d, $J = 8.0$ Hz, 1H), 5.97 (br s, 2H), 5.32 (s, 2H). MS m/z (ESI) 285 (M - H) $^+$. HPLC $t_R = 8.6$ min (system 1), 11.7 min (system 2).

5-(3-Fluorobenzoyloxy)quinazoline-2,4-diamine (5h). The crude product was purified by flash silica gel, eluted with 5–10% MeOH/DCM gradient, and dried in vacuo. Yield = 15%. ^1H NMR (400 MHz, DMSO- d_6) δ 7.51 (m, 2H), 7.36 (m, 2H), 7.31 (m, 2H), 7.22 (t, $J = 8.4, 0.8$ Hz, 1H), 7.10 (m, 1H), 6.72 (dd, $J = 8.4, 0.8$ Hz, 1H), 6.41 (d, $J = 7.6$ Hz, 1H), 5.96 (bs, 2H), 5.72 (q, $J = 6.4$ Hz, 1H), 1.69 (d, $J = 6.4$ Hz, 3H). MS m/z (ESI) 290 (M - H) $^+$. HPLC $t_R = 8.7$ min (system 1), 11.7 min (system 2).

5-(4-Fluorobenzoyloxy)quinazoline-2,4-diamine (5i). Yield = 38%. ^1H NMR (400 MHz, DMSO- d_6) δ 7.59 (m, 2H), 7.32 (t, 1H), 7.26 (m, 2H), 7.17 (br s, 2H), 6.77(dd, $J = 8.4, 0.8$ Hz, 1H), 6.61 (dd, $J = 7.6, 0.8$ Hz, 1H), 5.95 (br s, 2H), 5.25 (s, 2H). MS m/z (ESI) 285 (M + H) $^+$. HPLC $t_R = 8.8$ min (system 1), 11.8 min (system 2).

5-(Pyridin-3-ylmethoxy)quinazoline-2,4-diamine (5v). This compound was prepared starting from 3-pyridinylcarbinol as described for **5a** above. Yield = 24%. ^1H NMR (500 MHz, DMSO- d_6) δ 8.75 (d, $J = 1.5$ Hz, 1H), 8.57 (dd, $J = 1.0, 1.5$ Hz, 1H), 7.94 (d, $J = 8.0$ Hz, 1H), 7.45 (dd, $J = 5.0, 4.5$ Hz, 1H), 7.34 (t, $J = 8.0$ Hz, 1H), 7.17 (bs, 2H), 6.78 (d, $J = 8.5$ Hz, 1H), 6.64 (d, $J = 8.0$ Hz, 1H), 5.95 (s, 2H), 5.33 (s, 2H). MS m/z (ESI) 268 (M + H) $^+$. HPLC $t_R = 7.6$ min (system 1), 10.2 min (system 2).

5-(Thiophen-2-ylmethoxy)quinazoline-2,4-diamine (5w). Yield = 17%. ^1H NMR (500 MHz, DMSO- d_6) δ 7.62 (dd, $J = 5.3, 1.5$ Hz, 1H), 7.37 (t, $J = 6.5$ Hz, 1H), 7.3 (dd, $J = 3.3, 1.0$ Hz, 1H), 7.21 (s, 2H), 7.08 (dd, $J = 5.3, 4.0$ Hz, 1H), 6.8 (d, $J = 8.5$ Hz, 1H), 6.7 (d, $J = 8.0$ Hz, 1H), 5.96 (s, 2H), 5.45 (s, 2H). MS m/z (ESI) 273 (M + H) $^+$. HPLC $t_R = 8.3$ min (system 1), 11.3 min (system 2).

5-(Furan-2-ylmethoxy)quinazoline-2,4-diamine (5x). Yield = 5%. ^1H NMR (500 MHz, DMSO- d_6) δ 7.75 (s, 1H), 7.38 (t, $J = 8.5$ Hz, 1H), 7.17 (br d, 2H), 6.80 (d, $J = 8$ Hz, 1H), 7.72 (d, $J = 8$ Hz, 1H), 6.67 (d, $J = 3.5$ Hz, 1H), 6.51 (m, 1H), 5.97 (s, 2H), 5.24 (s, 2H). MS m/z 257 (M + H) $^+$ HPLC $t_R = 7.9$ min (system 1), 10.8 min (system 2).

5-(5-Methylisoxazol-3-ylmethoxy)quinazoline-2,4-diamine (5y). The target compound was prepared starting from (5-methylisoxazol-3-yl)methanol according to procedure A. Yield = 50%. ^1H NMR (500 MHz, DMSO- d_6) δ 7.40–7.20 (m, 3H), 6.81 (d, $J = 8.0$ Hz, 1H), 6.61 (d, $J = 7.5$ Hz, 1H), 6.35 (s, 3H), 5.96 (s, 2H), 5.33 (s, 2H), 2.43(s, 3H). MS m/z (ESI) 272 (M + H) $^+$. HPLC $t_R = 7.6$ min (system 1), 10.2 min (system 2).

5-(Quinolin-3-ylmethoxy)quinazoline-2,4-diamine (5z). Sodium borohydride (240 mg, 6.4 mmol) was added in portions to a solution of 3-quinolinecarboxaldehyde (910 mg, 5.8 mmol) in methanol at room temperature. After 3 h of stirring, the reaction mixture was quenched with 10 mL (aqueous) of saturated NH_4Cl . The mixture was extracted with ethyl acetate (3 \times 30 mL). Combined organics were washed with brine and dried over MgSO_4 . Crude quinolin-3-ylmethanol was obtained upon filtration and concentration in vacuo (795 mg, 86% yield). A solution of quinolin-3-ylmethanol (785 mg, 4.9 mmol) in DMF was added to a cooled (0 $^\circ\text{C}$) slurry of sodium hydride (1 equiv) in DMF under nitrogen atmosphere. The reaction mixture was slowly warmed to room temperature and stirred for 45 min. In another vessel, a solution of 2,6-difluorobenzonitrile (904 mg, 6.5 mmol) in DMF was chilled to 0 $^\circ\text{C}$, and sodium quinolin-3-ylmethoxide solution was added over 20 min. The mixture was then stirred for 2 h at room temperature. The reaction mixture was poured onto crushed ice–water, stirred, filtered, washed with water, and dried in vacuo to afford 2-fluoro-6-(quinolin-3-ylmethoxy)benzonitrile (1.1 g, 81% yield). 2-Fluoro-6-(quinolin-3-ylmethoxy)benzonitrile (300 mg, 1.1 mmol) and guanidine carbonate (1.1 mmol) were heated at 150 $^\circ\text{C}$ in dimethylacetamide for 5 h, then cooled back to room temperature overnight. The reaction mixture was diluted with water and stirred for 45 min, and the aqueous mixture was then extracted with ethyl acetate (6 \times 8 mL). Combined organic extracts were then washed with water (3 \times 5 mL) and brine and dried over MgSO_4 . Following filtration and concentration in vacuo, the material was purified by flash silica gel and eluted with 5–10% MeOH/DCM gradient to give 162 mg of 5-(quinolin-3-ylmethoxy)quinazoline-2,4-diamine (46% yield). ^1H NMR (400 MHz, DMSO- d_6) δ 9.09 (d, $J = 2.4$ Hz, 1H), 8.51 (d, $J = 2.4$ Hz, 1H), 8.03 (m, 2H), 7.80 (m, 1H), 7.65 (m, 1H), 7.36 (t, $J = 8.4, 8.0$ Hz, 1H), 7.21 (bs, 1H), 7.13 (bs, 1H), 6.80 (dd, $J = 0.8$ Hz, 1H), 6.72 (dd, $J = 0.8$ Hz, 1H), 5.95 (bs, 2H), 5.51 (s, 2H). MS m/z (ESI) 319 (M + H) $^+$.

General Procedure B: Preparation of 5-Nonaryl Ethers Derivatives of 2,4-Diaminoquinazolines 6a–m: 5-Methoxyquinazoline-2,4-diamine (6a). Sodium methoxide, 25 wt % in methanol (0.31 mL, 1.5 mmol), was added dropwise to a cooled (0 $^\circ\text{C}$) solution of 2,6-dinitrobenzonitrile (260.0 mg, 11.3 mmol) in DMF (1.5 mL) over 5 min. The reaction mixture was stirred at room temperature for 4½ h, poured onto crushed ice–water, filtered, and washed with water. The beige solid was recrystallized from ethanol to yield 173.0 mg of 2-methoxy-6-nitrobenzonitrile (67% yield). 2-Methoxy-6-nitrobenzonitrile (173.0 mg, 1 mmol), cyclohexene (0.33 mL, 3 mmol), and palladium, 10 wt %, on activated carbon (290 mg, 0.1 mmol) in ethanol (3.3 mL) were shaken at 80 $^\circ\text{C}$ for 7½ h. The reaction mixture was then diluted with ethanol (2.5 mL), filtered through a pad of Celite, washed with ethanol, and dried to afford 87.1 mg of 2-amino-6-methoxybenzonitrile (57% yield). 2-Amino-6-methoxybenzonitrile (608.1 mg, 4 mmol) and guanidine carbonate (825.6 mg, 4.6 mmol) were heated at 145 $^\circ\text{C}$ in dimethylacetamide (10 mL) for 7 h. The reaction mixture was diluted with water, stirred for 1 h, filtered, washed with water, and recrystallized with ethanol/water, 1:1, to yield 313.6 mg of 5-methoxyquinazoline-2,4-diamine (41% yield). ^1H NMR (400 MHz, DMSO- d_6) δ 7.35 (t, $J = 8.0$ Hz, 2H), 7.15 (bs, 1H), 6.76 (d, $J = 7.6$ Hz, 1H), 6.51 (d, $J = 8.0$ Hz, 1H), 5.89 (bs, 2H), 3.89

(s, 3H). MS *m/z* (ESI) 191 (M + H)⁺. Anal. (C₉H₁₀N₄O·0.5H₂O) C, H, N. HPLC *t_R* = 6.4 min (system 1), 8.6 min (system 2).

5-sec-Butoxyquinazoline-2,4-diamine (6g). Yield = 15%. ¹H NMR (500 MHz, DMSO-*d*₆) δ 7.34 (t, *J* = 8.0, 1H), 7.18 (s, 2H), 6.74 (d, *J* = 8.0 Hz, 1H), 6.55 (d, *J* = 8.0 Hz, 1H), 5.90 (s, 2H), 4.60 (m, 1H), 1.70 (m, 2H), 1.33 (d, *J* = 6.0 Hz, 3H), 0.95 (t, *J* = 7.0 Hz, 3H). MS *m/z* (ESI) 233 (M + H)⁺.

5-(Tetrahydropyran-2-ylmethoxy)quinazoline-2,4-diamine (6m). Yield = 58%. ¹H NMR (500 MHz, DMSO-*d*₆) δ 7.46 (s, 1H), 7.34 (t, *J* = 7.5 Hz, 1H), 7.21 (s, 1H), 6.77 (d, *J* = 8 Hz, 1H), 6.52 (d, *J* = 8 Hz, 1H), 5.95 (s, 2H), 4.15 (d, *J* = 9 Hz, 1H), 3.96 (m, 2H), 3.74 (s, 1H), 3.45 (t, *J* = 10 Hz, 1H), 1.82 (m, 1H), 1.51 (m, 5H). MS *m/z* (ESI) 275 (M + H)⁺.

General Procedure C: Synthesis of Racemic 5-(α -Substituted benzyl ether)-2,4-Diaminoquinazolines 7a-t. **5-[1-(3-Chlorophenyl)ethoxy]quinazoline-2,4-diamine (7a).** Sodium hydride (60%, 7.92 mmol) was suspended in DMF and cooled to 0 °C. 1-(3-Chlorophenyl)ethanol (1.24 g, 7.92 mmol) was dissolved in DMF and added dropwise to the sodium hydride mixture. The solution was allowed to warm to room temperature and stirred for 1 h. The solution was then cooled to 0 °C. 2,6-Difluorobenzonitrile (**2**) (0.9 equiv) in DMF was cooled to 0 °C, and the alcohol mixture was added dropwise to the benzonitrile solution and stirred for 2 h. The solution was poured over 100 mL of cooled water. The mixture was extracted with ethyl acetate and solvent removed to yield 1.94 g of 2-fluoro-6-[1-(3-chlorophenyl)ethoxy]benzonitrile (89% yield). 2-Fluoro-6-[1-(3-chlorophenyl)ethoxy]benzonitrile (137 mg, 0.5 mmol) and guanidine carbonate (216 mg, 1.2 mmol) were heated at 150 °C in dimethylacetamide for 6 h. The solvent was removed, and water was added. The resulting solid was filtered and dried in vacuo to yield 146 mg of 5-[3-(4-chlorophenyl)propoxy]quinazoline-2,4-diamine (93% yield). ¹H NMR (500 MHz, DMSO-*d*₆) δ 7.54 (d, *J* = 1.5 Hz, 1H), 7.36 (m, 3H), 7.29 (br s, 2H), 7.22 (t, *J* = 8.5 Hz, 1H), 6.72 (d, *J* = 8.0 Hz, 1H), 6.39 (d, *J* = 7.5 Hz, 1H), 5.99 (br s, 2H), 5.70 (q, *J* = 6.0 Hz, 1H), 1.68 (d, *J* = 6.5 Hz, 3H). ¹³C NMR (500 MHz, DMSO-*d*₆) δ 161.8, 160.6, 155.2, 155.0, 144.7, 133.3, 132.1, 130.6, 127.7, 125.7, 124.4, 117.2, 103.3, 101.6, 75.3. MS *m/z* 316 (M + H)⁺. FTIR 3494, 3471, 3447, 3306, 3098, 2971, 2923, 1650, 1610, 1566, 1507, 1474, 1447, 1432, 1400, 1372, 1352, 1337, 1327, 1245, 1203, 1073, 813, 779, 695. The sample was converted to the HCl salt using 4 N HCl in dioxane. Anal. (C₁₆H₁₅ClN₄O·HCl) C, H, N, Cl.

5-[1-(4-Chlorophenyl)ethoxy]quinazoline-2,4-diamine (7b). Sodium borohydride (26 mmol) was added portionwise to a cooled (0 °C) solution of 4-chloroacetophenone (2.0 g, 12.94 mmol) in ethanol under argon atmosphere. The reaction mixture was slowly warmed to room temperature and stirred for 4 h. The reaction was quenched with water, and the solvent was removed in vacuo. The sample was extracted with dichloromethane, washed with water and brine, and dried, and the solvent was removed to yield 2.0 g of 1-(4-chlorophenyl)ethanol (98% yield). A solution of 1-(4-chlorophenyl)ethanol (1.0 g, 6.39 mmol) was subsequently reacted using general procedure C as described above for synthesis of **7a** to provide the target compound **7b**. Yield = 44%. ¹H NMR (500 MHz, DMSO-*d*₆) δ 7.48 (d, *J* = 8.0 Hz, 2H), 7.43 (d, *J* = 8.5 Hz, 2H), 7.3 (brd, 2H), 7.21 (t, *J* = 8.5 Hz, 1H), 6.7 (d, *J* = 8.0 Hz, 1H), 6.38 (d, *J* = 8.5 Hz, 1H), 5.94 (s, 2H), 5.71 (q, *J* = 6.5 Hz, 1H), 1.67 (d, *J* = 6.5 Hz, 3H). MS *m/z* (ESI) 315 (M + H)⁺. HPLC *t_R* = 9.6 min (system 1), 12.7 min (system 2).

5-[1-(4-Chlorophenyl)propoxy]quinazoline-2,4-diamine (7c). Sodium borohydride (2 equiv) was added portionwise to a cooled (0 °C) solution of 4-chloropropiophenone (3.0 g, 17.79 mmol) in ethanol under argon atmosphere. The reaction mixture was slowly warmed to room temperature and stirred for 4 h. The reaction was quenched with water, and the solvent was removed. The sample was extracted with dichloromethane, washed with water and brine, and dried and the solvent was removed to yield 3.0 g of 1-(4-chlorophenyl)propanol (99% yield). The 1-(4-chlorophenyl)propanol (1.0 g, 5.86 mmol) was reacted following general procedure C, and the final product was isolated following purification by silica gel chromatography (5–10% methanol in dichlo-

romethane) to yield the desired product **7c**. Yield = 28%. ¹H NMR (500 MHz, DMSO-*d*₆) δ 7.44 (m, 4H), 7.35 (brd, 2H), 7.2 (t, *J* = 8.0 Hz, 1H), 6.69 (d, *J* = 7.5 Hz, 1H), 6.35 (d, *J* = 7.5 Hz, 1H), 5.99 (s, 2H), 5.48 (t, *J* = 7.0 Hz, 1H), 2.06 (m, 1H), 1.92 (m, 1H), 0.96 (t, *J* = 7.0 Hz, 3H). MS *m/z* (ESI) 330 (M + H)⁺. HPLC *t_R* = 10.0 min (system 1), 13.1 min (system 2).

5-[1-(4-Chlorophenyl)-2,2-dimethylpropoxy]quinazoline-2,4-diamine (7d). Grignard reaction of trimethylacetaldehyde (240.0 mg, 2.8 mmol) with 4-chlorophenylmagnesium bromide in anhydrous ether afforded 0.58 g of 1-(4-chlorophenyl)-2,2-dimethylpropanol (>100% yield). A solution of 1-(4-chlorophenyl)-2,2-dimethylpropanol (550.0 mg, 2.77 mmol) was subsequently reacted as described above for the synthesis of **7a** to provide the target compound. Purification by silica gel chromatography (5–10% methanol in dichloromethane) yielded 270 mg of 5-[1-(4-chlorophenyl)-2,2-dimethylpropoxy]quinazoline-2,4-diamine (67% yield). ¹H NMR (500 MHz, DMSO-*d*₆) δ 7.5 (brd, 2H), 7.4 (m, 4H), 7.17 (t, *J* = 8.0 Hz, 1H), 6.69 (d, *J* = 8.0 Hz, 1H), 6.31 (d, *J* = 7.5 Hz, 1H), 6.08 (s, 2H), 5.36 (s, 1H), 1.01 (s, 9H). MS *m/z* (ESI) 357 (M + H)⁺. HPLC *t_R* = 10.8 min (system 1), 13.8 min (system 2).

5-[1-(3-Trifluoromethylphenyl)ethoxy]quinazoline-2,4-diamine (7e). The α -methyl-3-(trifluoromethyl)benzyl alcohol (0.6 mL, 3.9 mmol) was used for the synthesis using general procedure C to provide the desired product **7e**. Yield = 13%. ¹H NMR (400 MHz, DMSO-*d*₆) δ 7.85 (s, 1H), 7.76 (d, *J* = 7.2 Hz, 1H), 7.65 (m, 2H), 7.38 (bs, 1H), 7.3 (bs, 1H), 7.21 (t, *J* = 8.4 Hz, 1H), 6.72 (dd, *J* = 0.8, 8.4 Hz, 1H), 6.41 (d, *J* = 7.6 Hz, 1H), 5.97 (bs, 2H), 5.83 (m, 1H), 1.72 (d, *J* = 6.4 Hz, 3H). MS *m/z* (ESI) 350 (M + H)⁺. HPLC *t_R* = 9.7 min (system 1), 12.7 min (system 2).

5-[1-(3-Fluorophenyl)ethoxy]quinazoline-2,4-diamine (7f). Yield = 43%. ¹H NMR (400 MHz, DMSO-*d*₆) δ 7.42 (m, 3H), 7.31 (m, 2H), 7.22 (t, *J* = 8.4, 8 Hz, 1H), 7.11 (m, 1H), 6.72 (dd, *J* = 0.8 Hz, 1H), 6.41 (d, *J* = 7.6 Hz, 1H), 5.96 (bs, 2H), 5.72 (q, *J* = 6.4 Hz, 1H), 1.69 (d, *J* = 6.4 Hz, 3H). MS (ESI) *m/z* 300 (M + H)⁺. HPLC *t_R* = 9.0 min (system 1), 12.0 min (system 2).

5-[1-(3,5-Difluorophenyl)ethoxy]quinazoline-2,4-diamine (7g). Sodium borohydride (267 mg, 7.0 mmol) was added in portions to a solution of 3,5-difluoroacetophenone (1 g, 6.4 mmol) in methanol at room temperature. After 3 h of being stirred, the reaction mixture was quenched with 10 mL (aqueous) saturated NH₄Cl. The mixture was extracted with ethyl acetate (3 × 30 mL). Combined organics were washed with brine and dried over MgSO₄. Crude 3,5-difluorophenylethanol was obtained upon filtration and concentration in vacuo to a colorless oil (960 mg, 95% yield). A solution of 3,5-difluorophenylethanol (960 mg, 6.1 mmol) was subsequently reacted following general procedure C. The crude product was purified by flash silica gel and eluted with 5–10% MeOH/DCM gradient to provide 145 mg of 5-[1-(3,5-difluorophenyl)-1-methylethoxy]quinazoline-2,4-diamine (42% yield). ¹H NMR (400 MHz, DMSO-*d*₆) δ 7.31 (bs, 2H), 7.24 (m, 2H), 7.15 (m, 1H), 6.74 (dd, *J* = 8.0, 7.6 Hz, 1H), 6.40 (d, *J* = 7.6 Hz, 1H), 5.97 (bs, 2H), 5.72 (q, *J* = 6.4 Hz, 1H), 1.69 (d, *J* = 6.4 Hz, 3H). MS *m/z* (ESI) 315 (M + H)⁺. HPLC *t_R* = 9.2 min (system 1), 12.2 min (system 2).

5-[1-(4-Fluorophenyl)-1-methylethoxy]quinazoline-2,4-diamine (7j). The crude product was purified by flash silica gel and eluted with 5–10% MeOH/DCM gradient. 5-[1-(4-Fluorophenyl)-1-methylethoxy]quinazoline-2,4-diamine was obtained in a 77% yield (275 mg). ¹H NMR (400 MHz, DMSO-*d*₆) δ 7.51 (m, 2H), 7.4 (bs, 1H), 7.3 (bs, 1H), 7.19 (m, 3H), 7.2 (bs, 1H), 6.72 (dd, *J* = 8.4, 0.8 Hz, 1H), 6.43 (d, *J* = 7.6 Hz, 1H), 5.99 (bs, 2H), 5.72 (q, *J* = 6.4 Hz, 1H), 1.68 (d, *J* = 6.4 Hz, 3H). MS *m/z* (ESI) 297 (M + H)⁺. HPLC *t_R* = 9.012.0 min (system 1), 11.6 min (system 2).

5-[1-(4-Trifluoromethylphenyl)ethoxy]quinazoline-2,4-diamine (7k). The material was purified by flash silica gel and eluted with 5–10% MeOH/DCM gradient to give 177 mg (34% yield) of 5-[1-methyl-1-(4-trifluoromethylphenyl)ethoxy]quinazoline-2,4-diamine. ¹H NMR (400 MHz, DMSO-*d*₆) δ 7.76 (d, *J* = 8.4 Hz, 2H), 7.68 (d, *J* = 8.4 Hz, 2H), 7.37 (bs, 1H), 7.3 (bs, 1H), 7.2 (t, *J* = 8.4, 8.0 Hz, 1H), 6.72 (dd, *J* = 8.4, 0.8 Hz, 1H), 6.36 (d, *J* = 7.2 Hz, 1H), 5.97 (bs, 2H), 5.72 (q, *J* = 6.0 Hz, 1H), 1.71 (d, *J* =

6.4 Hz, 3H). MS m/z (ESI) 347 (M - H)⁺. HPLC t_R = 9.8 min (system 1), 12.7 min (system 2).

5-((S)-1-Naphthalen-2-ylethoxy)quinazoline-2,4-diamine (7s). General procedure C was used. Commercially available (S)-(-)- α -methyl-2-naphthalene methanol was used as the starting material. Following purification by flash silica gel and elution with 5–10% MeOH/DCM gradient, 310 mg of 5-((S)-1-naphthalen-2-ylethoxy)quinazoline-2,4-diamine (37% yield) was obtained. ¹H NMR (500 MHz, DMSO- d_6) δ 7.97 (s, 1H), 7.94 (d, J = 8.0 Hz, 1H), 7.89 (m, 2H), 7.61 (m, 1H), 7.51 (m, 3H), 7.29 (bs, 1H), 7.18 (t, J = 8.5, 8.0 Hz, 1H), 6.69 (d, J = 8.5 Hz, 1H), 6.47 (d, J = 8.0 Hz, 1H), 5.95 (bs, 2H), 5.85 (q, J = 6.5 Hz, 1H), 1.78 (d, J = 6.5 Hz, 3H). ¹³C NMR (500 MHz, DMSO- d_6) δ 161.9, 160.6, 155.3, 155.1, 139.5, 132.7, 132.5, 132.1, 128.5, 127.8, 127.6, 126.4, 126.1, 124.6, 123.6, 117.0, 103.5, 101.7, 76.4, 23.7. MS m/z (ESI) 332 (M + H)⁺.

5-(1-Naphthalen-1-ylethoxy)quinazoline-2,4-diamine (7t). The racemic α -methyl-1-naphthalene methanol (1.0 g, 5.8 mmol) was used for the synthesis of this target analogue, and general procedure C was utilized. Purification by flash silica gel and following elution with 5–10% MeOH/DCM gradient provided 65 mg of 5-(1-naphthalen-1-yl-ethoxy)quinazoline-2,4-diamine (17% yield). ¹H NMR (400 MHz, DMSO- d_6) δ 8.32 (d, J = 8.4 Hz, 1H), 7.98 (d, J = 8.0 Hz, 1H), 7.85 (d, J = 8.0 Hz, 1H), 7.56 (m, 6H), 7.12 (t, J = 8.0 Hz, 1H), 6.67 (d, J = 9.2 Hz, 1H), 6.45 (m, 1H), 6.22 (d, J = 7.6 Hz, 1H), 6.0 (br s, 2H), 1.81 (s, 3H). MS m/z (ESI) 331 (M - H)⁺.

5-[(R)-1-(3-Chlorophenyl)ethoxy]quinazolin-2,4-diamine, ((R)-7a). To a solution of borane–tetrahydrofuran (0.647 mL, 0.647 mmol, Aldrich, 1 M solution in THF) and (S)-MeCBS (0.647 mL, 0.647 mmol, Aldrich, 1 M solution in toluene) was added simultaneously a solution of 3-chloroacetophenone (1.00 g, 6.47 mmol) in anhydrous tetrahydrofuran (2.42 mL) and a solution of borane–tetrahydrofuran (3.24 mL, 3.24 mmol, Aldrich, 1 M solution in THF) over 30 min at ambient temperature. After complete addition, the reaction mixture was stirred for 10 min, quenched slowly at 0 °C with methanol (0.94 mL) and then saturated HCl in ether (0.12 mL). After being stirred at 0 °C for 5 min and ambient temperature for 30 min, the solution was concentrated in vacuo to an oil. The oil was twice diluted with benzene and concentrated in vacuo, diluted with ether, and concentrated in vacuo to an oil. Purification by flash chromatography (silica gel, 20% ethyl acetate in hexane) provided (R)-1-(3-chlorophenyl)ethanol as a clear colorless oil (0.784 g, 78% yield). Optical rotation in CHCl₃ at 20 °C at concentration 0.220 was +40.9° (literature: +44°).⁴⁵ A solution of (R)-1-(3-chlorophenyl)ethanol (0.730 g, 4.66 mmol) in DMF (5 mL) was added to a 0 °C slurry of sodium hydride (0.207 g, 5.18 mmol) in DMF (5 mL) under nitrogen atmosphere. The reaction mixture was warmed to room temperature, stirred for 3 h, and then cooled with an ice bath. The cold orange solution was added dropwise to a 0 °C solution of 2,6-difluorobenzonitrile (0.720 g, 5.18 mmol) in DMF (5 mL). After the mixture was stirred at ambient temperature for 18 h, the mixture was diluted with water and extracted with ethyl acetate. The organic layer was washed with water and brine, dried over MgSO₄, and concentrated in vacuo to a yellow semisolid. Flash chromatography purification (silica gel, 50% hexane in DCM) afforded the 2-fluoro-5-[(R)-1-(3-chlorophenyl)ethoxy]benzonitrile as a pale-yellow oil (0.645 g, 50% yield). A mixture of 2-fluoro-5-[(R)-1-(3-chlorophenyl)ethoxy]benzonitrile (0.630 g, 2.29 mmol) and guanidine carbonate (0.988 g, 5.48 mmol) in dimethylacetamide (4.0 mL) was heated at 145 °C for 7 h. The mixture was concentrated in vacuo to a black solid. The solid was stirred in a mixture of water and ethyl acetate, and then the tan solid was collected by filtration in vacuo. Flash chromatography purification (silica gel, 10% methanol in DCM) afforded 5-(R)-1-(3-chlorophenyl)ethoxyquinazoline-2,4-diamine as an off-white solid (0.357 g, 49% yield). ¹H NMR (400 MHz, DMSO- d_6) δ 7.54 (d, J = 1.6 Hz, 1H), 7.32–7.44 (m, 5H), 7.23 (t, J = 8.4 Hz), 6.72 (dd, J = 8.4, 0.8 Hz, 1H), 6.41 (d, J = 8.0 Hz, 1H), 6.03 (s, 2H), 5.71 (q, J = 6.4 Hz, 1H), 1.68 (d, J =

6.4 Hz, 3H). MS (ESI) m/z 315 (M + H)⁺. HPLC t_R = 9.5 min (system 1), 12.6 min (system 2), chiral 99.8% ee, t_R = 26.22 min.

5-[(S)-1-(3-Chlorophenyl)ethoxy]quinazolin-2,4-diamine ((S)-7a). To a solution of borane–tetrahydrofuran (77.6 mL, 77.62 mmol, Aldrich, 1 M solution in THF) and (R)-MeCBS (12.9 mL, 12.9 mmol, Aldrich, 1 M solution in toluene) was added a solution of 3-chloroacetophenone (20.0 g, 129.37 mmol) in anhydrous tetrahydrofuran slowly over 30 min at room temperature. After complete addition, the reaction mixture was stirred for 10 min and quenched with 2 N hydrochloric acid over 30 min. The reaction mixture was extracted with ether, dried, filtered, and concentrated in vacuo to afford 20.8 g of (S)-1-(3-chlorophenyl)ethanol as a viscous liquid (>100% yield). A solution of (S)-1-(3-chlorophenyl)ethanol (20.4 g, 130.26 mmol) in DMF was reacted as described above from the (R)-enantiomer ((R)-7a). The crude white solid isolated following reaction with guanidine carbonate step was recrystallized from methanol–water to yield 24.9 g of 5-(S)-1-(3-chlorophenyl)ethoxyquinazoline-2,4-diamine (75% yield). ¹H NMR (400 MHz, DMSO- d_6) δ 7.55 (d, J = 1.6 Hz, 1H), 7.31–7.43 (m, 5H), 7.23 (t, J = 7.2 Hz), 6.74 (dd, J = 8.4, 0.8 Hz, 1H), 6.39 (d, J = 8.0 Hz, 1H), 6.05 (s, 2H), 5.7 (q, J = 6.4 Hz, 1H), 1.69 (d, J = 6.4 Hz, 3H). ¹³C NMR (100.5 MHz, DMSO- d_6) δ 161.87, 160.62, 155.17, 155.03, 144.7, 133.31, 132.18, 130.64, 127.68, 125.72, 124.42, 117.16, 103.33, 101.62, 75.37, 23.68. MS m/z (ESI) 315 (M + H)⁺. FT-IR 3509, 3392, 3350, 3308, 3164, 3134, 1642, 1590, 1569, 1550, 1499, 1443, 1252, 1075, 814 cm⁻¹. Mp 224–225 °C. Chiral HPLC (99.0% ee), t_R = 21.99 min. Anal. (C₁₆H₁₅ClN₄O) C, H, N.

5-(1-Phenylethoxy)quinazoline-2,4-diamine ((RS)-7u). Sodium hydride (60%, 316 mg, 7.9 mmol) was suspended in DMF and cooled to 0 °C. Starting with *sec*-phenethyl alcohol (966 mg, 7.9 mmol), synthesis of the target compound was carried out following general procedure C described for 7a. The desired product was isolated following recrystallization from ethanol/water to yield 49 mg of 5-(1-phenylethoxy)quinazoline-2,4-diamine (35% yield). ¹H NMR (500 MHz, DMSO- d_6) δ 7.44 (d, J = 7 Hz, 2H), 7.37 (m, 3H), 7.27 (m, 2H), 7.20 (t, J = 8.5 Hz, 1H), 6.69 (d, J = 8 Hz, 1H), 6.41 (d, J = 7.5 Hz, 1H), 5.93 (s, 2H), 5.68 (q, J = 6 Hz, 1H), 1.37 (d, J = 6.5 Hz, 3H). MS m/z (ESI) 281 (M + H)⁺. HPLC t_R = 8.9 min (system 1), 11.9 min (system 2).

5-((R)-1-Phenylethoxy)quinazoline-2,4-diamine ((R)-7u). Starting with (R)-*sec*-phenethyl alcohol (0.33 mL, 4.1 mmol) and following the procedure described above for the racemic product (7u), 115 mg of 5-((R)-1-phenylethoxy)quinazoline-2,4-diamine (21% yield) was isolated. ¹H NMR (400 MHz, DMSO- d_6) δ 7.44 (m, 3H), 7.23 (t, J = 8.0 Hz, 2H), 7.02 (dd, J = 7.2, 4.2 Hz, 1H), 6.71 (dd, J = 7.6, 0.8 Hz, 1H), 6.42 (d, J = 7.2 Hz, 1H), 6.19 (bs, 2H), 5.95 (bs, 2H), 5.69 (m, 1H), 1.68 (d, J = 6.4 Hz, 3H). MS m/z (ESI) 281 (M + H)⁺.

5-((S)-1-Phenylethoxy)quinazoline-2,4-diamine ((S)-7u). Following the procedure described above for ((R)-7u) enantiomer, (S)-*sec*-phenethyl alcohol (611 mg, 5 mmol) provided 429 mg of 5-((S)-1-phenylethoxy)quinazoline-2,4-diamine (77% yield). ¹H NMR (400 MHz, DMSO- d_6) δ 7.92 (s, 1H), 7.44 (m, 7H), 6.70 (dd, J = 8.4, 0.8 Hz, 1 H), 6.43 (d, J = 7.6 Hz, 1H), 6.03 (br s, 2H), 5.69 (q, J = 6.4 Hz, 1H), 1.67 (d, J = 6.4 Hz, 3H). MS m/z (ESI) 281 (M + H)⁺. HPLC t_R = 8.9 min (system 1), 12.0 min (system 2).

5-[1-(3-Chlorophenyl)-1-methylethoxy]quinazoline-2,4-diamine (8a). To a cooled (–10 °C) and stirred solution of 3-chloroacetophenone (1.5 g, 9.7 mmol) in anhydrous ether (20 mL) was added dropwise methylmagnesium bromide (3.6 mL, 10.67 mmol, Aldrich, 3 M solution in ether). The reaction mixture was slowly warmed to room temperature and stirred for 20 h. It was cooled to 0 °C, and the reaction was quenched with saturated ammonium chloride solution (6 mL). The sample was extracted with ethyl acetate, washed with brine, dried, and concentrated in vacuo to afford 1.55 g of 2-(3-chlorophenyl)propan-2-ol (94% yield). 2-(3-Chlorophenyl)propan-2-ol (0.8 g, 4.69 mmol) was reacted using general procedure A. The crude product from step 2 was purified by silica gel column chromatography using 5% methanol in dichloromethane to afford 88 mg of 5-[1-(3-chlorophe-

nyl)-1-methylethoxy]quinazoline-2,4-diamine (26% yield). ^1H NMR (400 MHz, $\text{DMSO-}d_6$) δ 7.38–7.56 (m, 6H), 7.08 (t, $J = 8.8$ Hz, 1H), 6.7 (d, $J = 9.6$ Hz, 1H), 6.05 (s, 2H), 5.8 (d, $J = 8.4$ Hz, 1H), 1.81 (s, 6H). MS m/z (ESI) 329 ($\text{M} + \text{H}$) $^+$. HPLC $t_R = 9.7$ min (system 1), 13.0 min (system 2).

5-[1-(3-Chlorophenyl)cyclohexyloxy]quinazoline-2,4-diamine (8b). To a cooled (0 °C) and stirred solution of cyclohexanone (0.3 g, 3.1 mmol) in anhydrous THF (10 mL) was added dropwise 3-chlorophenylmagnesium bromide (3.4 mL, 10.67 mmol, Aldrich, 1 M solution in THF). The reaction mixture was slowly warmed to room temperature and stirred for 20 h. It was cooled to 0 °C, and the reaction was quenched with saturated ammonium chloride solution (4 mL). The sample was extracted with ethyl acetate, washed with brine, dried, and concentrated in vacuo to afford 0.55 g of 1-(3-chlorophenyl)cyclohexanol (>100% yield). 1-(3-Chlorophenyl)cyclohexanol (0.5 g, 2.84 mmol) was reacted using general procedure A. The crude product from step 2 was purified by silica gel column chromatography using 10% methanol in dichloromethane, giving 40 mg of 5-[1-(3-chlorophenyl)cyclohexyloxy]quinazoline-2,4-diamine (24% yield). ^1H NMR (400 MHz, $\text{DMSO-}d_6$) δ 7.52–7.59 (m, 2H), 7.36–7.46 (m, 4H), 7.02 (t, $J = 8.0$ Hz, 1H), 6.66 (dd, $J = 8.4$, 0.8 Hz, 1H), 5.94 (s, 2H), 5.76 (dd, $J = 8.2$, 1.2 Hz, 1H), 2.42 (m, 3H), 1.88–2.01 (m, 2H), 1.45–1.68 (m, 4H), 1.35–1.42 (m, 1H). MS m/z (APCI) 269 ($\text{M} + \text{H}$) $^+$.

5-[1-(3-Chlorophenyl)cyclopropoxy]quinazoline-2,4-diamine (8c). To a heated (50 °C) and vigorously stirred suspension of samarium powder (1.0 g, 6.65 mmol) in anhydrous THF (3 mL) were added dropwise a solution of methyl 3-chlorobenzoate (0.27 g, 1.58 mmol) and diiodomethane (1.27 g, 4.74 mmol) over 1.5 h. The reaction mixture was stirred at room temperature for 1 h, cooled to –10 °C, and then quenched with 1 N HCl solution (6 mL). The sample was extracted with ether, washed with brine, dried, and concentrated in vacuo. Purification by silica gel column chromatography using 1:1 DCM–Hex afforded 0.1 g of 1-(3-chlorophenyl)cyclopropanol (37% yield). 1-(3-Chlorophenyl)cyclopropanol (0.09 g, 0.53 mmol) was reacted using general procedure A. The crude product from step 2 was purified by silica gel column chromatography using 5–10% methanol in dichloromethane to afford 30 mg of 5-[1-(3-chlorophenyl)cyclopropoxy]quinazoline-2,4-diamine (54% yield). ^1H NMR (400 MHz, $\text{DMSO-}d_6$) δ 7.67 (s, 2H), 7.53–7.58 (m, 1H), 7.26–7.46 (m, 3H), 6.84 (dd, $J = 8.2$, 0.8 Hz, 1H), 6.41 (s, 2H), 6.32–6.4 (m, 2H), 1.72 (d, $J = 7.2$ Hz, 4H). MS m/z (ESI) 327 ($\text{M} + \text{H}$) $^+$. HPLC $t_R = 9.8$ min (system 1), 13.0 min (system 2).

5-(6-Chloroindan-1-yloxy)quinazoline-2,4-diamine (9a). 3-(4-Chlorophenyl)propionic acid (3.83 g, 20.7 mmol) was dissolved in 50 mL of thionyl chloride and stirred at room temperature overnight. The excess thionyl chloride is removed in vacuo to give 3-(4-chlorophenyl)propionyl chloride as a pale-yellow oil, which was used without purification (4.21 g, ~100% yield). 3-(4-Chlorophenyl)propionyl chloride (4.21 g, 20.7 mmol) dissolved in 25 mL of dichloromethane was slowly added to a cold (0 °C), stirred suspension of aluminum chloride (2.77 g, 20.7 mmol) in 75 mL of dichloromethane. After being stirred for 10 min at 0 °C, the reaction mixture was heated to reflux for 4 h and then cooled to room temperature overnight. The mixture was diluted with 100 mL of water, and the layers were separated. The organic layer was washed with 0.1 M sodium hydroxide and brine and then dried over magnesium sulfate. The dried solution is concentrated in vacuo to give 2.51 g of 6-chloroindan-1-one (72% yield). Sodium borohydride (1.1 equiv) was added portionwise to a solution of 6-chloroindan-1-one (2.51 g, 15 mmol) in methanol. The reaction mixture was stirred overnight at room temperature and then quenched with water and extracted with ethyl acetate. Solvent was removed in vacuo to yield 2.03 g of 6-chloroindan-1-ol (80% yield). 6-Chloroindan-1-ol (2.11 g, 12.5 mmol) was dissolved in DMF and added dropwise to a stirred suspension of sodium hydride (60%, 1 equiv) in DMF at 0 °C. The solution was allowed to warm to room temperature and stirred for 1 h. The solution was then cooled to 0 °C. 2,6-Difluorobenzonitrile (0.9 equiv) in DMF was cooled to 0

°C, and the alcohol mixture was added dropwise to the benzonitrile solution and stirred for 2 h. The solution was poured over 100 mL of ice-cooled water. The solution was stored in the refrigerator for 3 h and solid was collected by filtration and dried in vacuo to yield 2.97 g of 2-(6-chloroindan-1-yloxy)-6-fluorobenzonitrile (76% yield). 2-(6-Chloroindan-1-yloxy)-6-fluorobenzonitrile (2.91 g, 10 mmol) was dissolved in dimethylacetamide (100 mL) with guanidine carbonate (3.82 g, 21 mmol). The vessel was purged with N_2 , sealed, and heated to 150 °C for 8 h and then cooled to room temperature overnight. The reaction solution was slowly diluted with 150 mL of water and stirred 1 h, then refrigerated for 1 h to form a fine brown precipitate that was removed by filtration in vacuo, washed with ethanol, and dried overnight under high vacuum (10 Torr) at 30 °C. The dry solids were slurried in boiling methanol and filtered while hot to give 1.22 g of 5-(6-chloroindan-1-yloxy)quinazoline-2,4-diamine (30% yield). ^1H NMR (500 MHz, $\text{DMSO-}d_6$) δ 7.55 (s, 1H), 7.41 (t, $J = 8.0$ Hz, 1H), 7.41 (s, 1H), 7.11 (br s, 1H), 6.96 (br s, 1H), 6.82 (d, $J = 8.5$ Hz, 1H), 6.77 (d, $J = 8.0$ Hz, 1H), 6.01 (s, 3H), 3.06 (m, 1H), 2.92 (m, 1H), 2.68 (m, 1H), 2.17 (m, 1H). ^{13}C NMR (500 MHz, $\text{DMSO-}d_6$) δ 161.8, 160.6, 155.5, 155.2, 143.3, 143.0, 132.4, 131.2, 129.1, 126.8, 124.9, 117.3, 103.1, 101.7, 81.6, 31.9, 29.3. MS m/z (ESI) 410 ($\text{M} + \text{H}$) $^+$. HPLC $t_R = 9.9$ min (system 1), 16.1 min (system 2). FT-IR 3505, 3385, 3306, 3116, 2989, 2955, 2911, 1646, 1613, 1589, 1573, 1558, 1499, 1478, 1442, 1430, 1403, 1354, 1345, 1282, 1247, 1216, 1175, 1062, 813 cm^{-1} .

5-(4-Chloroindan-1-yloxy)quinazoline-2,4-diamine (9b). 4-Chloro-1-indanone (689.8 mg, 4.1 mmol) was stirred in methanol (4 mL) and cooled to 0 °C. Sodium borohydride (156.6 mg, 4.1 mmol) was added in small portions at 0 °C, and the mixture was stirred at 0 °C for ½ h. Water (5 mL) was added to the reaction mixture when lots of white foam formed. The mixture was neutralized with saturated ammonium chloride (10 mL). The solid was filtered, washed with water, and dried in vacuo to obtain 630.9 mg of white solid as 4-chloro-1-indanol (90% yield). 4-Chloro-1-indanol (596 mg, 3.5 mmol) was reacted as described for **9a** to provide the crude product that was purified by column chromatography with DCM/methanol, 9:1, to yield 90.9 mg of 5-(4-chloroindan-1-yloxy)quinazoline-2,4-diamine (16% yield). ^1H NMR (400 MHz, $\text{DMSO-}d_6$) δ 7.46 (dd, $J = 8.4$, 16.8 Hz, 3H), 7.35 (t, $J = 8.0$ Hz, 1H), 7.25 (bs, 1H), 7.05 (bs, 1H), 6.83 (m, 2H), 6.18 (s, 2H), 6.11 (m, 1H), 3.10 (m, 1H), 2.98 (m, 1H), 2.74 (m, 1H), 2.19 (m, 1H). MS m/z (ESI) 327 ($\text{M} + \text{H}$) $^+$. HPLC $t_R = 9.9$ min (system 1), 13.2 min (system 2).

General Procedure D: Synthesis of 5-(Aryloxymethyl)quinazoline-2,4-diamine (10a–i). **5-(3-Chlorophenoxymethyl)quinazoline-2,4-diamine (10a).** 3-Chlorophenol (0.27 g, 2.07 mmol) and potassium carbonate (1 equiv) were added to a cooled (0 °C) and stirred solution of 2-bromomethyl-6-nitrobenzonitrile⁴⁴ (0.5 g, 2.07 mmol) in DMF under nitrogen atmosphere. The reaction mixture was stirred at 0 °C for 1.5 h, then diluted with pyridine (1.5 mL) and water, stirred for 1 h, filtered, and dried in vacuo. Purification by silica gel chromatography (1:1 dichloromethane in hexanes) yielded 185 mg of 2-(3-chlorophenoxymethyl)-6-nitrobenzonitrile (31% yield). A solution of tin(II) chloride (0.4 g, 1.73 mmol) and concentrated hydrochloric acid (1.2 mL) was cooled (15 °C), and a solution of 2-(3-chlorophenoxymethyl)-6-nitrobenzonitrile (100.0 mg, 0.35 mmol) was added while stirring. The reaction mixture was slowly warmed to room temperature and stirred for 3 h. The reaction mixture was poured over crushed ice and potassium hydroxide solution. The mixture was stirred, extracted with dichloromethane, filtered, and concentrated in vacuo. Purification by silica gel chromatography (dichloromethane) yielded 38 mg of 2-amino-6-(3-chlorophenoxymethyl)benzonitrile (43% yield). 2-Amino-6-(3-chlorophenoxymethyl)benzonitrile (35.0 mg, 0.14 mmol) and chloroformamide hydrochloride (23.0 mg, 0.2 mmol) were heated at 140 °C in diglyme for 3 h. The reaction mixture was diluted with water, stirred for 2 h, filtered, washed with water, and concentrated in vacuo. Purification by silica gel chromatography (5–10% methanol in dichloromethane) yielded 20 mg of 5-(3-chlorophenoxymethyl)quinazoline-2,4-diamine (48% yield). HPLC

$t_R = 9.3$ min (system 1), 12.5 min (system 2). $^1\text{H NMR}$ (400 MHz, $\text{DMSO}-d_6$) δ 7.5 (dd, $J = 8.6, 7.2$ Hz, 1H), 7.37 (t, $J = 8.4$ Hz, 1H), 7.27 (m, 2H), 7.21 (d, $J = 6.0$ Hz, 1H), 7.07–7.12 (m, 2H), 6.91 (s, 2H), 6.27 (s, 2H), 5.44 (s, 2H). MS m/z (ESI) 301 ($\text{M} + \text{H}$) $^+$.

5-(2-Chlorophenoxy)methylquinazoline-2,4-diamine (10b). The target compound was prepared from 2-chlorophenol (0.11 g, 0.83 mmol) using general procedure D. Purification by silica gel chromatography (5% methanol in dichloromethane) yielded 50 mg of 5-(2-chlorophenoxy)methylquinazoline-2,4-diamine (54% yield). $^1\text{H NMR}$ (400 MHz, $\text{DMSO}-d_6$) δ 7.44–7.5 (m, 3H), 7.36 (ddd, $J = 8.0, 8.0, 1.6$ Hz, 1H), 7.26 (dd, $J = 8.4, 1.2$ Hz, 1H), 7.21 (dd, $J = 8.4, 1.2$ Hz, 1H), 7.04 (ddd, $J = 7.6, 7.6, 1.6$ Hz, 1H), 6.93 (s, 2H), 6.14 (s, 2H), 5.51 (s, 2H). MS m/z (ESI) 301 ($\text{M} + \text{H}$) $^+$. HPLC $t_R = 8.9$ min (system 1), 12.2 min (system 2).

5-(2-Iodophenoxy)methylquinazoline-2,4-diamine (10c). The target compound was prepared from 2-iodophenol (0.18 g, 0.87 mmol) following general procedure D. Purification by silica gel chromatography (5% methanol in dichloromethane) yielded 65 mg (49%) of **10c**. $^1\text{H NMR}$ (400 MHz, $\text{DMSO}-d_6$) δ 7.82 (d, $J = 7.6$ Hz, 1H), 7.49 (t, $J = 7.6$ Hz, 1H), 7.42 (t, $J = 7.2$ Hz, 1H), 7.27 (m, 3H), 6.86 (m, 3H), 6.16 (s, 2H), 5.47 (s, 2H). MS m/z (ESI) 393 ($\text{M} + \text{H}$) $^+$. HPLC $t_R = 9.3$ min (system 1), 12.6 min (system 2).

5-(2-Fluorophenoxy)methylquinazoline-2,4-diamine (10d). The target compound was prepared from 2-fluorophenol (0.07 g, 0.62 mmol) following general procedure D. Purification by silica gel chromatography (5% methanol in dichloromethane) yielded 65 mg (46%) of **10d**. $^1\text{H NMR}$ (400 MHz, $\text{DMSO}-d_6$) δ 7.42–7.48 (m, 2H), 7.22–7.29 (m, 2H), 7.13–7.2 (m, 2H), 6.99–7.06 (m, 1H), 6.94 (s, 2H), 6.14 (s, 2H), 5.48 (s, 2H). MS m/z (ESI) 286 ($\text{M} + \text{H}$) $^+$. HPLC $t_R = 8.6$ min (system 1), 11.6 min (system 2).

5-(2,4-Difluorophenoxy)methylquinazoline-2,4-diamine (10i). The target compound was prepared from 2,4-difluorophenol (0.11 g, 0.83 mmol) following general procedure D. Purification by silica gel chromatography (5% methanol in dichloromethane) yielded 72 mg (52%) of **10i**. $^1\text{H NMR}$ (400 MHz, $\text{DMSO}-d_6$) δ 7.43–7.51 (m, 2H), 7.3–7.38 (m, 1H), 7.27 (dd, $J = 8.4, 1.2$ Hz, 1H), 7.14 (d, $J = 6.8$ Hz, 1H), 7.05–7.11 (m, 1H), 7.04 (s, 2H), 6.25 (s, 2H), 5.47 (s, 2H). MS m/z (ESI) 303 ($\text{M} + \text{H}$) $^+$.

Synthesis of 5-(Piperidin-4-ylmethoxy)quinazoline-2,4-diamine (31). 4-Piperidinmethanol **27** (1.5 g, 13.0 mmol) was dissolved in a mixture of dichloromethane and triethylamine (2.7 mL, 19.5 mmol). Di-*tert*-butyl dicarbonate (3.1 g, 14.3 mmol) was added and stirred for 2.5 h at room temperature. The mixture was poured over dilute acetic acid, and the organic layer was separated. Organics were washed with water, saturated sodium bicarbonate and brine, dried over MgSO_4 , and concentrated in vacuo. Crude material was purified by flash chromatography using 1–5% methanol/DCM gradient to afford 4-hydroxymethylpiperidine-1-carboxylic acid *tert*-butyl ester **28** (2.5 g, 89% yield). A solution of 4-hydroxymethylpiperidine-1-carboxylic acid *tert*-butyl ester (1 g, 4.6 mmol) in DMF was added dropwise to a suspension of sodium hydride (60%, 1 equiv) in DMF that was cooled to 0 °C. The solution was allowed to warm to room temperature and stirred for 1 h. 2,6-Difluorobenzonitrile **2** (0.9 equiv) in DMF was cooled to 0 °C, and the alcohol mixture was added dropwise to the benzonitrile solution and stirred for 2 h. The solution was poured over 100 mL of cooled water. The solution was stored in the refrigerator for 3 h, and the solid was collected by filtration. 4-(2-Cyano-3-fluorophenoxy)methylpiperidine-1-carboxylic acid *tert*-butyl ester **29** (1.22 g, 81% yield) was obtained after purification by column chromatography (15–20% ethyl acetate/hexanes gradient). The cyclization of 4-(2-cyano-3-fluorophenoxy)methylpiperidine-1-carboxylic acid *tert*-butyl ester **29** (17.9 g, 53.5 mmol) was carried out using guanidine carbonate (53.5 mmol) and heating at 140 °C in dimethylacetamide for 4 h. The mixture was cooled and triturated with water for 45 min. Solids were filtered off and triturated with ethanol. Solids were collected by filtration and dried in vacuo to afford 16.4 g of 4-(2,4-diaminoquinazolin-5-ylloxymethyl)piperidine-1-carboxylic acid *tert*-butyl ester **30** (82% yield).

4-(2,4-Diaminoquinazolin-5-ylloxymethyl)piperidine-1-carboxylic acid *tert*-butyl ester (16.4 g, 44.0 mmol) was suspended in 80 mL of dioxane, and 4 M HCl in dioxane (176 mL, 176 mmol) was added, changing the mixture from homogeneous to heterogeneous. After the mixture was stirred for 5 h at room temperature, solids were filtered off and rinsed once with ether. Solids were triturated with 1 N NaOH for 30 min. Solids were collected by filtration and dried in vacuo to yield 5-(piperidin-4-ylmethoxy)quinazoline-2,4-diamine **31** (9.05 g, 75% yield).

General Procedure E: Functionalization of 5-(Piperidin-4-ylmethoxy)quinazoline-2,4-diamine. To a mixture of 5-(piperidin-4-ylmethoxy)quinazoline-2,4-diamine (**31**) (4.4 mmol, 1 equiv) and triethylamine (1.2 mL, 8.8 mmol, 2 equiv) in 10 mL of DMF was added a benzyl halide (4.8 mmole, 1.1 equiv), and the mixture was stirred at 60 °C for 16 h. The mixture was cooled to room temperature and concentrated in vacuo. Residue was taken up in 30 mL of dichloromethane and 2 mL of methanol, creating a homogeneous mixture. Product **11** was purified via flash chromatography using a 5–10% MeOH/DCM with 0.1% NH_4OH gradient. Material was then repurified by trituration with 1 N NaOH and ethanol for 1.5 h.

[5-(1-(2-Fluorobenzyl)piperidin-4-ylmethoxy)quinazoline-2,4-diamine (11a). The title compound was prepared using general procedure E from **31** and 2-fluorobenzyl bromide (0.6 mL, 4.8 mmol), and solids were collected by filtration and dried in vacuo to obtain 5-[(1-(2-fluorobenzyl)piperidin-4-ylmethoxy)quinazoline-2,4-diamine, 740 mg (44% yield). $^1\text{H NMR}$ (500 MHz, $\text{DMSO}-d_6$) δ 7.40 (t, $J = 7.5$ Hz, 1H), 7.31 (m, 1H), 7.18 (m, 3H), 6.77 (d, $J = 8.0$ Hz, 1H), 6.52 (d, $J = 8.0$ Hz, 1H), 5.98 (br s, 2H), 3.97 (d, $J = 6.0$ Hz, 2H), 3.53 (s, 2H), 2.85 (br d, $J = 11.5$ Hz, 2H), 2.01 (t, $J = 10$ Hz, 2H), 1.84 (m, 1H), 1.73 (d, $J = 12$ Hz, 2H), 1.34 (m, 2H). MS m/z (ESI) 382 ($\text{M} + \text{H}$) $^+$. Anal. ($\text{C}_{21}\text{H}_{24}\text{FN}_5\text{O}$) C, H, N.

5-[1-(3-Chlorobenzyl)piperidin-4-ylmethoxy]quinazoline-2,4-diamine (11b). The title compound employing general procedure E was prepared using 3-chlorobenzyl bromide in DMF (4 mL). The crude solid was purified by silica gel column chromatography using 3–10% methanol in dichloromethane to afford 1.82 g of 5-[1-(3-chlorobenzyl)piperidin-4-ylmethoxy]quinazoline-2,4-diamine (50% yield). HPLC $t_R = 7.5$ min (system 1), 10.2 min (system 2). $^1\text{H NMR}$ (400 MHz, $\text{DMSO}-d_6$) δ 7.25–7.38 (m, 5H), 7.2 (s, 2H), 6.77 (dd, $J = 8.0, 1.2$ Hz, 1H), 6.53 (dd, $J = 8.0, 0.8$ Hz, 1H), 5.95 (s, 2H), 3.99 (d, $J = 6.4$ Hz, 2H), 3.48 (s, 2H), 2.84 (d, $J = 11.2$ Hz, 2H), 1.7–2.07 (m, 5H), 1.3–1.42 (m, 2H). MS m/z (ESI) 399 ($\text{M} + \text{H}$) $^+$.

[5-(1-(2-Chlorobenzyl)piperidin-4-ylmethoxy)quinazoline-2,4-diamine (11c). The title compound employing general procedure E was prepared using 2-chlorobenzyl bromide (0.5 mL, 3.7 mmol) in DMF (4 mL). Solids were filtered off, rinsed once with methanol and twice with diethyl ether, and dried in vacuo to yield the title compound (684 mg, 47% yield). $^1\text{H NMR}$ (400 MHz, $\text{DMSO}-d_6$) δ 7.49 (d, $J = 7.6$ Hz, 1H), 7.41 (d, $J = 7.6$ Hz, 1H), 7.32 (m, 3H), 7.2 (br s, 2H), 6.76 (d, $J = 7.6$ Hz, 1H), 6.53 (d, $J = 7.6$ Hz, 1H), 5.94 (br s, 2H), 3.99 (d, $J = 6.0$ Hz, 2H), 3.57 (s, 2H), 2.89 (m, 2H), 2.08 (t, $J = 12$ Hz, 2H), 1.89 (m, 1H), 1.75 (d, $J = 12$ Hz, 2H), 1.36 (m, 2H). MS m/z (ESI) 398 ($\text{M} + \text{H}$) $^+$.

General Procedure F: Functionalization of 5-(Piperidin-4-ylmethoxy)quinazoline-2,4-diamine Using Polymer-Bound Reagents: 5-[1-(4-Chlorobenzyl)piperidin-4-ylmethoxy]quinazoline-2,4-diamine Hydrochloride (11d). 5-(Piperidin-4-ylmethoxy)quinazoline-2,4-diamine (75 mg, 0.27 mmol) (**31**) was shaken for 60 h at 60 °C in the presence of 3-(morpholinyl)propylpolystyrene sulfonamide (PS-NMM) (240 mg, 0.6 mmol) and 3,4-difluorobenzyl bromide (66 mg, 0.32 mmol) in 4 mL *N,N*-DMF. Tris-(2-aminoethyl)aminomethyl polystyrene (PS-trisamine) (168 mg, 0.6 mmol) was then added to the mixture, and shaking was continued for an additional 2 h. Resins were filtered off and rinsed with methanol. The filtrate was concentrated in vacuo, and the residue was triturated with 2 mL of 1 N NaOH and ethanol (1:1). Solids were collected by filtration to yield 5-[1-(3,4-difluorobenzyl)piperidin-4-ylmethoxy]quinazoline-2,4-diamine, which was stirred in

the presence of 4 M HCl in dioxane (4 equiv). Solids were filtered, rinsed once with ether, and dried in vacuo to give 5-[1-(4-chlorobenzyl)piperidin-4-ylmethoxy]quinazoline-2,4-diamine hydrochloride (66 mg, 56% yield). ¹H NMR (400 MHz, DMSO-*d*₆) δ 12.9 (s, 1H), 11.3 (s, 1H), 8.82 (s, 1H), 8.23 (s, 1H), 7.7 (m, 4H), 7.52 (d, *J* = 6.8 Hz, 2H), 7.02 (m, 2H), 4.66 (br s, 3H), 4.26 (d, *J* = 4.8 Hz, 2H), 4.17 (d, *J* = 6.4 Hz, 2H), 3.34 (br d, *J* = 11.6 Hz, 2H), 2.87 (m, 2H), 2.2 (m, 1H), 1.81 (m, 4H). MS *m/z* (ESI) 398 (M + H)⁺.

5-[1-(1-Naphthalen-1-ylmethyl)piperidin-4-ylmethoxy]quinazoline-2,4-diamine (11e). The title compound employing general procedure F was prepared using 1-(chloromethyl)naphthalene (57 mg, 0.32 mmol) in 4 mL of DMF to yield 94 mg (84% yield). ¹H NMR (400 MHz, DMSO-*d*₆) δ 8.26 (d, *J* = 8.0 Hz, 1H), 7.85 (m, 2H), 7.53 (m, 3H), 7.44 (d, *J* = 4.8 Hz, 1H), 7.33 (t, *J* = 8.4 Hz, 1H), 7.19 (br s, 2H), 6.75 (d, *J* = 8.4 Hz, 2H), 6.51 (d, *J* = 8.0 Hz, 1H), 5.94 (br s, 2H), 3.79 (d, *J* = 6.4 Hz, 2H), 3.87 (s, 2H), 2.92 (d, *J* = 11.2 Hz, 2H), 2.07 (t, *J* = 11.6 Hz, 2H), 1.91 (m, 1H), 1.74 (d, *J* = 12.4 Hz, 2H), 1.3 (m, 2H). MS *m/z* (ESI) 414 (M + H)⁺.

5-[1-(2-Naphthalen-1-ylmethyl)piperidin-4-ylmethoxy]quinazoline-2,4-diamine (11f). The title compound employing general procedure F was prepared using 2-(bromomethyl)naphthalene (77 mg, 0.35 mmol) in 4 mL of DMF to yield 75 mg (67% yield). ¹H NMR (400 MHz, DMSO-*d*₆) δ 7.88 (m, 3H), 7.79 (s, 1H), 7.48 (m, 3H), 7.34 (t, *J* = 8.0 Hz, 1H), 7.22 (br s, 2H), 6.76 (d, *J* = 8.0 Hz, 1H), 6.53 (d, *J* = 7.6 Hz, 1H), 5.96 (br s, 2H), 3.99 (d, *J* = 6.0 Hz, 2H), 3.64 (s, 2H), 2.92 (m, 2H), 2.03 (t, *J* = 10.8 Hz, 2H), 1.91 (m, 1H), 1.74 (d, *J* = 12.0 Hz, 2H), 1.37 (m, 2H). MS *m/z* (ESI) 414 (M + H)⁺.

[4-(2,4-Diaminoquinazolin-5-ylloxymethyl)piperidin-1-yl](2-fluorophenyl)methanone (12a). The title compound employing general procedure F was prepared using 2-fluorobenzoyl chloride (57 mg, 0.36 mmol) in 4 mL of DMF to yield 43 mg (60%). ¹H NMR (400 MHz, DMSO-*d*₆) δ 7.49 (m, 1H), 7.33 (m, 4H), 7.17 (br s, 2H), 6.77 (d, *J* = 8.0 Hz, 1H), 6.54 (d, *J* = 8.0 Hz, 1H), 5.94 (br s, 2H), 4.56 (br d, *J* = 12.8 Hz, 1H), 4.03 (d, *J* = 6.0 Hz, 2H), 3.42 (br d, *J* = 12.8 Hz, 1H), 3.12 (m, 1H), 2.86 (t, *J* = 11.2 Hz, 1H), 2.22 (br s, 1H), 1.89 (br d, *J* = 13.6 Hz, 1H), 1.73 (br d, *J* = 11.2 Hz, 1H), 1.26 (m, 2H). MS *m/z* (ESI) 396 (M + H)⁺.

(3-Chlorophenyl)-[4-(2,4-diaminoquinazolin-5-ylloxymethyl)piperidin-1-yl]methanone (12b). 2-Fluoro-6-(piperidin-1-ylmethoxy)benzoxonitrile hydrochloride (0.7 mmol) was suspended in 2 mL of tetrahydrofuran, and in one portion triethylamine was added (0.3 mL, 2.2 mmol) to the mixture at room temperature. 3-Chlorobenzoyl chloride (129 mg, 0.7 mmol) was then added, and the mixture was stirred at room temperature for 16 h. Reaction was quenched with 2 mL of 1 N HCl. The mixture was extracted twice with 10 mL of ethyl acetate, and organic layers were combined. The mixture was then washed with saturated NaHCO₃ and brine and dried over MgSO₄. The mixture was filtered and concentrated in vacuo to an oil. Material was purified via flash silica gel chromatography using 0.5–2% methanol/dichloromethane gradient to afford 200 mg of 2-[1-(3-chlorobenzoyl)piperidin-4-ylmethoxy-6-fluorobenzonitrile (77% yield). The cyclization of 2-[1-(3-chlorobenzoyl)piperidin-4-ylmethoxy-6-fluorobenzonitrile (194 mg, 0.5 mmol) was carried out using guanidine carbonate (1 equiv mmol) and heating at 140 °C in dimethylacetamide for 4 h. The mixture was cooled and triturated with water for 45 min. Solids were filtered off and triturated with ethanol. Solids were collected by filtration and dried in vacuo to afford 169 mg of (3-chlorophenyl)-[4-(2,4-diaminoquinazolin-5-ylloxymethyl)piperidin-1-yl]methanone (82% yield). HPLC *t_R* = 8.9 min (system 1), 12.3 min (system 2). ¹H NMR (400 MHz, DMSO-*d*₆) δ 7.51 (m, 3H), 7.35 (m, 2H), 7.19 (br d, *J* = 16.4 Hz, 2H), 6.77 (dd, *J* = 8.4, 0.8 Hz, 1H), 6.57 (d, *J* = 8.0 Hz, 1H), 5.98 (br s, 2H), 4.51 (br s, 1H), 4.03 (d, *J* = 6.4 Hz, 2H), 3.55 (br s, 1H), 3.11 (m, 1H), 2.84 (br s, 1H), 2.22 (m, 1H), 1.88 (br s, 1H), 1.75 (br s, 1H), 1.33 (br s, 2H). MS *m/z* (ESI) 412 (M – H)⁺.

[5-(1-(2-Fluorobenzenesulfonyl)piperidin-4-ylmethoxy]quinazoline-2,4-diamine (13a). The title compound employing general procedure E was prepared using 2-fluorobenzenesulfonyl chloride (196 mg, 1.0 mmol) in 2.5 mL of DMF to yield crude product (331 mg, 85% yield). Following purification by silica gel column (5% MeOH/CH₂Cl₂ + 1% NH₄OH), the fractions containing the desired product were reduced in vacuo to ~5 mL and diluted with 2 M HCl in Et₂O (5 mL). The solvents were completely removed under N₂ purge. The resulting semisolid was triturated with absolute EtOH and stored at 2 °C for 72 h. The resulting solids were filtered and dried under vacuum at 30 °C overnight to yield 182 mg of 5-[1-(2-fluorobenzenesulfonyl)piperidin-4-ylmethoxy]quinazoline-2,4-diamine hydrochloride (yield = 43%). ¹H NMR (500 MHz, DMSO-*d*₆) δ 12.93 (s, 1H), 8.95 (s, 1H), 8.16 (s, 1H), 7.80 (t, *J* = 7.5 Hz, 1H), 7.77 (dt, *J* = 7.5, 2.5 Hz, 1H), 7.68 (t, *J* = 8.5 Hz, 1H), 7.50 (t, *J* = 8.5 Hz, 1H), 7.45 (t, *J* = 7.5 Hz, 1H), 6.99 (d, *J* = 8.5 Hz, 1H), 4.14 (d, *J* = 6.5 Hz, 2H), 3.74 (br d, *J* = 12.0 Hz, 2H), 2.54 (m, 2H), 2.07 (m, 1H), 1.84 (br d, *J* = 12 Hz, 2H), 1.33 (m, 2H). ¹³C NMR (500 MHz, DMSO-*d*₆) δ 162.3, 159.2, 157.2, 156.8, 154.2, 141.0, 136.2, 135.8, 130.8, 125.1, 124.2, 117.6, 117.5, 108.6, 106.8, 99.6, 73.1, 45.1, 33.4, 27.8. MS *m/z* (ESI) 432 (M + H)⁺.

5-[4-(3-Chlorobenzenesulfonyl)piperidin-4-ylmethoxy]quinazoline-2,4-diamine (13b). Compound **31** (50 mg, 0.18 mmol) was shaken for 60 h at room temperature in the presence of 3-(morpholino)propylpolystyrene sulfonamide (PS-NMM) (160 mg, 0.4 mmol) and 3-chlorobenzenesulfonyl chloride (78 mg, 0.37 mmol) in 4 mL of DMF. Tris-(2-aminoethyl)aminomethyl polystyrene (PS-trisamine) (112 mg, 0.4 mmol) was then added to the mixture, and shaking was continued for an additional 2 h. Resins were filtered off and rinsed with methanol. Filtrate was concentrated at reduced pressure, and residue was triturated with 2 mL of 1 N NaOH and ethanol (1:1). Solids were collected by filtration and dried in vacuo to yield 80 mg of 5-[4-(3-chlorobenzenesulfonyl)piperidin-4-ylmethoxy]quinazoline-2,4-diamine (99% yield). ¹H NMR (400 MHz, DMSO-*d*₆) δ 7.82 (m, 1H), 7.72 (m, 3H), 7.32 (t, *J* = 8.4 Hz, 1H), 7.11 (br s, 2H), 6.75 (d, *J* = 8.0 Hz, 1H), 6.50 (d, *J* = 7.6 Hz, 1H), 5.93 (br s, 2H), 3.96 (d, *J* = 6.4 Hz, 2H), 3.72 (br d, *J* = 11.6 Hz, 2H), 2.32 (t, *J* = 12 Hz, 2H), 1.84 (m, 3H), 1.36 (m, 2H). MS *m/z* (ESI) 448 (M + H)⁺.

Biological Assays. *SMN2* Promoter Assay. (NSC-34/β-Lactamase Assay). The 3.4 kb *SMN2* promoter NSC-34/β-lactamase assay developed by Jarecki et al.³³ was used with the following modifications. In brief, 55 000 cells/well were plated into a 96-well cell culture plate and incubated along with test compounds for 19 h at 37 °C, 90% humidity, and 5% CO₂. The total assay volume was 100 μL. Test compound concentrations were varied, usually in the concentration range 2 pM to 90 μM (dose curves). At the end of the incubation, 14 μL of CCF2/AM (dye, purchased from Invitrogen)⁴⁶ was added to each of the assay wells and the assay plates were incubated for another 3 h before the plates are read on a fluorometer (LJL Analyst). The CCF2/AM dye was prepared according to an assay kit from Invitrogen (K1085). The resulting raw data were processed using IDBS activity base to determine EC₅₀ values and other curve parameters. For each sample, there are two readouts: the substrate at 520 nm (green) and the product at 450 nm (blue). The ratio of the blue to the green signal for each sample was calculated, and this value was then divided by a similar value calculated for the negative control (which contains no compound). The resulting value is called fold induction (FoldInd) and was plotted against compound concentration to generate a dose curve. TSA (trichostatin A, a histone deacetylase inhibitor) was used as a positive control during the initial stages of the project and was subsequently replaced with compound **2b** as the SAR elaboration continued. The EC₅₀ for each curve is calculated from the curve along with other curve parameters, including maximum fold induction (MaxFoldInd, MFI), which is the maximum induction apparent on the curve.

DHFR Assay. The assay is an adaptation for 96-well plate format from Appleman et al.⁴⁷ Human, recombinant dihydrofolate reductase (Sigma, D6566) was incubated along with test compounds (119

pM to 125 μ M) and NADPH (Sigma, N-7505) in 96-well plates. After a 10 min preincubation at room temperature, dihydrofolic acid (Sigma, D7006) was added and the kinetic traces at 340 nm were measured on a Spectra Max 190 plate reader at room temperature. Reaction rates were determined from the slopes of the linear portions of the progress curves. The final assay conditions were 0.014 units of DHFR, 300 μ M NADPH, 30 μ M dihydrofolic acid, 50 mM Tris, pH 7.6, 100 mM NaCl, and 1.25% DMSO. Each compound was measured in duplicate on every assay plate. Each assay plate contained 12 positive controls (DMSO only) and 12 negative controls (no dihydrofolic acid). All data were percent-normalized with respect to controls and presented as percent inhibition. Inhibition data were analyzed using Prism and fit to a standard four-parameter logistic equation to calculate IC₅₀ values.

In Vitro Studies Using NSC-34 Murine Cell Line. Test compound and TSA (trichostatin A, Sigma, T-8552) were formulated in DMSO and added to NSC-34 cell culture for final concentrations of 500 nM, 50 nM (test compound), and 100 nM (TSA), respectively. Final concentration of DMSO was 0.5%. The cells were incubated for 18 h and then harvested for RNA isolation using RNeasy Mini Kit (Qiagen) according to the manufacturer's protocol. RNA quality and quantity were measured on an Agilent 2100 bioanalyzer (Agilent Technologies). cDNA synthesis was performed using High Capacity cDNA Archive kit (Applied Biosystems) according to the manufacturer's protocol. Gene expression analysis was performed using TaqMan Assays-on-Demand Gene Expression Products (Applied Biosystems) according to the manufacturer's protocol (SMN assay no. Mm00488315_m1). Each assay was run in triplicate, and the data were normalized against an internal housekeeping gene, B-actin (ACTB assay no. 4352933E). The relative difference in expression was calculated using the expression $2e(-\Delta C_T)$. Statistical comparisons between groups in the gene expression studies were performed using Student's *t* test, and an associated probability of <5% was considered significant.

Biochemical Analysis in SMA Patient Fibroblasts. Cell lines derived from skin fibroblasts of a type I SMA patient (line 3813) and from a SMA carrier (line 3814) have been described previously.⁴⁸ For immunoblot analyses, cells were plated into 12-well plates at a density of 4000 cells/cm². For immunofluorescence experiments, cells were seeded onto glass coverslips coated with 1% gelatin at a density of 4000 cells/cm². Drug compounds or DMSO was added to medium at a 1:1000 dilution. Medium was changed daily, and fresh compound was added. Immunoblot of fibroblast extracts was performed as described previously.¹¹ Sixty micrograms of protein extract were loaded per lane of a 12% polyacrylamide gel. The primary antibodies used in these experiments were a mouse anti-SMN mAb (MANSMA2 (8F7),⁴⁹ 1:100) and a mouse anti- β -tubulin mAb (Tub2.1, Sigma-Aldrich, 1:1000). Immunostaining of fibroblast cells was accomplished as described previously⁴⁸ with modification. Briefly, cells grown on gelatinized coverslips were fixed with fixative buffer⁵⁰ (2% paraformaldehyde, 400 μ M CaCl₂, 50 mM sucrose in 100 mM sodium phosphate buffer, pH 7.4) for 30 min at room temperature, rinsed with phosphate buffered saline (PBS), and permeabilized with ice-cold acetone for 10 min. After drying for at least 30 min at room temperature, the cells were rehydrated with PBS for 10 min and then blocked with 5 \times BLOCK⁴⁸ (5% horse serum, 5% fetal bovine serum, and 0.1% bovine serum albumin in PBS) for 60 min at room temperature. The cells were incubated overnight with primary antibody solution (mouse anti-SMN MANSMA 2, diluted 1:200 in 1 \times BLOCK) at 4 $^{\circ}$ C. The cells were then washed (3 \times 10 min) with PBS and incubated with secondary antibody solution (biotinylated goat antimouse IgG (Jackson ImmunoResearch) diluted 1:400 with 1 \times BLOCK) for 60 min at room temperature. The cells were then washed with PBS (3 \times 10 min) and then incubated with AlexaFluor 594-conjugated streptavidin (Invitrogen) diluted 1:200 with PBS for 60 min at room temperature. Cells were then counterstained with Hoescht 33342 (1 μ g/mL) in PBS for 5 min. After thorough washing with PBS, coverslips were mounted onto glass slides with ImmuMount (Shandon Lipshaw) and stored at 4 $^{\circ}$ C until analysis.

For gem counting, immunolabeling was visualized using a Nikon fluorescent microscope, and the number of gems in 100 randomly selected nuclei and the number of cells with gems were collected. Confocal images were obtained using a Zeiss 510 META laser scanning confocal microscope (Campus Microscopy and Imaging Facility, The Ohio State University) as a series of optic sections (thickness of 500 nm/section) taken through the *z*-axis. These stacks of sections were then compressed using LSM 5 image browser (Carl Zeiss, Inc.).

Statistical Analysis. All parametric data were expressed as mean standard error. Comparisons made between parametric data were made using one-way ANOVA with a Bonferonni post hoc test. All statistical analyses were performed using SPSS, version 14.

Pharmacokinetics in Mice. NMRI mice were dosed using the formulation and dose as indicated, and plasma and brain samples at the time indicated were processed.

Plasma Sample Processing. An aliquot of 50 μ L of plasma sample was pipetted into a 96-well plate. A solution (150 μ L) of ice-cold acetonitrile containing internal standard was added to each sample. The plate was vortex-mixed for 3 min and then allowed to stand for 30 min in a refrigerator (2–8 $^{\circ}$ C). Samples were centrifuged for 10 min at 4100 rpm. The supernatant (130 μ L) from each sample was transferred to new 96-well plates, and 130 μ L of mobile phase was added to the supernatant and vortex-mixed for 3 min. Subsequently, the solutions were centrifuged for 10 min at 4100 rpm and an amount of 20 μ L of each supernatant was injected into the LC–MS–MS system for quantification. Concentration of a given compound in plasma is reported as ng/mL.

Brain Sample Processing. Two volumes (mL) of ringer acetate were added for each gram of brain tissue. The brain tissue sample was homogenized using a Tissue-Tearor hand-held homogenizer (BioSpec Products, OK). The sample was homogenized for 30 s in an ice–water bath. The homogenized brain tissue (2.5 mL sample from each 1 g of brain tissues) was transferred to an Eppendorf tube and stored in a –25 $^{\circ}$ C freezer until analyzed. After thawing at room temperature, an aliquot of 50 μ L of homogenized brain was pipetted into a 96-well plate. A solution (150 μ L) of ice-cold acetonitrile containing internal standard was added to each sample. The plate was vortex-mixed for 3 min and then allowed to stand for 30 min in a refrigerator (2–8 $^{\circ}$ C). These samples were then processed as described above for plasma samples. Concentration of the compound in brain is reported as ng/g. All pharmacokinetic parameters reported were calculated using WinNoLin (version 5.0).

Computational Chemistry and Molecular Modeling Methods. Conformational Analysis. The 2D molecular models of molecules **1c**, **2b**, **4a**, **6a**, and **6b** were constructed using ISIS draw, and a small structure data file (sd) was generated. This sd file was then subjected to CONCORD 6.0 in the SYBYL7.0³⁹ environment, and 3D structures were generated. The energy minimization of all the molecules were carried out using MMFF94 with conjugate gradient method having a gradient norm of 0.001 kcal/mol. Gasteiger–Huckel charges were assigned to all the molecules. All the minimized structures were aligned by atom-to-atom map of the common ether oxygen and quinazoline core atoms. The conformational search analysis of all the above molecules was performed in SYBYL7.0 using the Systematic Search module. All rotatable bonds (RB) were analyzed, and they were given a torsional increment angle of 10 $^{\circ}$. The “compute energy” and the “electrostatic” options incorporated in the systematic search were used to generate the conformers with an energy cutoff of 7.0 kcal/mol. At the same time, the coordinate maps were generated assigning the origin and the target atomic centers (as shown in Figure 3). Finally, for all conformations within 3.0 kcal/mol from the lowest energy conformer, a sweep graph was created by defining the trajectory type with the sequence of atoms and the vectors maps were generated.

Analysis of the human DHFR Cocrystal Structure. The human DHFR-bound ligand (1s3u.pdb) from Protein Data Bank was analyzed in SYBYL7.0. Atom type and the bond type for the bound ligand were modified as needed. By use of the BIOPOLYMER module of SYBYL7.0, all hydrogen atoms were added to the protein

and the ligand. All nonhydrogen atoms were defined as an aggregate, and hydrogens were minimized using the TRIPOS force field. The hydrogen bonding network was created between the bound ligand and the interacting residues in the active site.

Acknowledgment. The authors gratefully acknowledge the scientific contributions of Denise Anderson for running mass spectral analyses, Dr. Jun Zhang and Emmanuel Onua for ADME support, Dr. Nelson Zhao and Amanda Heimann for acquiring NMR spectra, Kevin Schilling and Brian Bock for performing analytical HPLC analyses, and Jim Nie for carrying out chiral HPLC analyses. We also thank Dr. Glenn E. Morris for generously providing us with the MANSMA2 (8F7) mouse anti-SMN antibody, and we thank the Campus Microscopy and Imaging Facility (The Ohio State University) for providing access to the confocal microscope. The authors also thank Drs. Jill Jarecki, Christopher Spancake, David Zembower, Brent Stockwell, and Brian Pollok for helpful discussions and Audrey Lewis for her enthusiastic encouragement of this work. The project was supported in its entirety by funding from the Families of SMA.

Supporting Information Available: Synthetic procedures for compounds **1g–i**, **5d,j–u**, **6c–f,h,j–l**, **7m–r**, **10e–h,j–k**, **11g–m**, **12c–m**, **13c–k**; table listing HPLC retention times and purity data; assay details for *SMN2* promoter assay; assay description for metabolic stability. This material is available free of charge via the Internet at <http://pubs.acs.org>.

References

- Pears, J. Incidence, prevalence, and gene frequency studies of chronic childhood spinal muscular atrophy. *J. Med. Genet.* **1978**, *15*, 409–413.
- Roberts, D. F.; Chavez, J.; Court, S. D. The genetic component in child mortality. *Arch. Dis. Child.* **1970**, *45*, 33–38.
- McAndrew, P. E.; Parsons, D. W.; Simard, L. R.; Rochette, C.; Ray, P. N.; Mendell, J. R.; Prior, T. W.; Burghes, A. H. Identification of proximal spinal muscular atrophy carriers and patients by analysis of SMN1 and SMN2 gene copy number. *Am. J. Hum. Genet.* **1997**, *60*, 1411–1422.
- Lefebvre, S.; Burglen, L.; Reboullet, S.; Clermont, O.; Burlet, P.; Viollet, L.; Benichou, B.; Cruaud, C.; Millasseau, P.; Zeviani, M.; et al. Identification and characterization of a spinal muscular atrophy-determining gene. *Cell* **1995**, *80*, 155–165.
- Lorson, C. L.; Hahnen, E.; Androphy, E. J.; Wirth, B. A single nucleotide in the SMN gene regulates splicing and is responsible for spinal muscular atrophy. *Proc. Natl. Acad. Sci. U.S.A.* **1999**, *96*, 6307–6311.
- Monani, U. R.; Lorson, C. L.; Parsons, D. W.; Prior, T. W.; Androphy, E. J.; Burghes, A. H.; McPherson, J. D. A single nucleotide difference that alters splicing patterns distinguishes the SMA gene SMN1 from the copy gene SMN2. *Hum. Mol. Genet.* **1999**, *8*, 1177–1183.
- Cartegni, L.; Krainer, A. R. Disruption of an SF2/ASF-dependent exonic splicing enhancer in SMN2 causes spinal muscular atrophy in the absence of SMN1. *Nat. Genet.* **2002**, *30*, 377–384.
- Gennarelli, M.; Lucarelli, M.; Capon, F.; Pizzuti, A.; Merlini, L.; Angelini, C.; Novelli, G.; Dallapiccola, B. Survival motor neuron gene transcript analysis in muscle from spinal muscular atrophy patients. *Biochem. Biophys. Res. Commun.* **1995**, *213*, 342–348.
- Lorson, C. L.; Strasswimmer, J.; Yao, J. M.; Baleja, J. D.; Hahnen, E.; Wirth, B.; Le, T.; Burghes, A. H.; Androphy, E. J. SMN oligomerization defect correlates with spinal muscular atrophy severity. *Nat. Genet.* **1998**, *19*, 63–66.
- Lorson, C. L.; Androphy, E. J. An exonic enhancer is required for inclusion of an essential exon in the SMA-determining gene SMN. *Hum. Mol. Genet.* **2000**, *9*, 259–265.
- Covert, D. D.; Le, T. T.; McAndrew, P. E.; Strasswimmer, J.; Crawford, T. O.; Mendell, J. R.; Coulson, S. E.; Androphy, E. J.; Prior, T. W.; Burghes, A. H. The survival motor neuron protein in spinal muscular atrophy. *Hum. Mol. Genet.* **1997**, *6*, 1205–1214.
- Lefebvre, S.; Burlet, P.; Liu, Q.; Bertrand, S.; Clermont, O.; Munnich, A.; Dreyfuss, G.; Melki, J. Correlation between severity and SMN protein level in spinal muscular atrophy. *Nat. Genet.* **1997**, *16*, 265–269.
- Vitali, T.; Sossi, V.; Tiziano, F.; Zappata, S.; Giuli, A.; Paravatou-Petsotas, M.; Neri, G.; Brahe, C. Detection of the survival motor neuron (SMN) genes by FISH: further evidence for a role for SMN2 in the modulation of disease severity in SMA patients. *Hum. Mol. Genet.* **1999**, *8*, 2525–2532.
- Campbell, L.; Potter, A.; Ignatius, J.; Dubowitz, V.; Davies, K. Genomic variation and gene conversion in spinal muscular atrophy: implications for disease process and clinical phenotype. *Am. J. Hum. Genet.* **1997**, *61*, 40–50.
- Feldkotter, M.; Schwarzer, V.; Wirth, R.; Wienker, T. F.; Wirth, B. Quantitative analyses of SMN1 and SMN2 based on real-time light Cycler PCR: fast and highly reliable carrier testing and prediction of severity of spinal muscular atrophy. *Am. J. Hum. Genet.* **2002**, *70*, 358–368.
- Arklblad, E. L.; Darin, N.; Berg, K.; Kimber, E.; Brandberg, G.; Lindberg, H.; Holmberg, E.; Tulinius, M.; Nordling, M. Multiplex ligation-dependent probe amplification improves diagnostics in spinal muscular atrophy. *Neuromuscular Disord.* **2006**, *16*, 830–838.
- DiDonato, C. J.; Chen, X.; Noya, D.; Kroenberg, J. R.; Nadeau, J.; Simard, L. R. Cloning, characterization, and copy number of the murine survival motor neuron gene: homolog of the spinal muscular atrophy-determining gene. *Genome Res.* **1997**, *7*, 339–351.
- Viollet, L.; Bertrand, S.; Brunialti, A. L.; Lefebvre, S.; Burlet, P.; Clermont, O.; Cruaud, C.; Guenet, J. L.; Munnich, A.; Melki, J. cDNA isolation, expression, and chromosomal localization of the mouse survival motor neuron gene (*Smn*). *Genomics* **1997**, *40*, 185–188.
- Schrank, B.; Gotz, R.; Gunnerson, J. M.; Ure, J. M.; Toyka, K.; Smith, A.; Sendtner, M. Inactivation of the survival motor neuron gene, a candidate gene for human spinal muscular atrophy, leads to massive cell death in early mouse embryos. *Proc. Natl. Acad. Sci. U.S.A.* **1997**, *94*, 9920–9925.
- Vitte, J. M.; Davoult, B.; Natacha Roblot, N.; Mayer, M.; Joshi, V.; Courageot, S.; Tronche, F.; Vadrot, J.; Moreau, M. H.; Kemeny, F.; Melki, J. Deletion of murine *Smn* exon 7 directed to liver leads to severe defect of liver development associated with iron overload. *Am. J. Pathol.* **2004**, *165*, 1731–1741.
- Cifuentes-Diaz, C.; Frugier, T.; Tiziano, F. D.; Lacene, E.; Roblot, N.; Joshi, V.; Moreau, M. H.; Melki, J. Deletion of murine SMN exon 7 directed to skeletal muscle leads to severe muscular dystrophy. *J. Cell Biol.* **2001**, *152*, 1107–1114.
- Frugier, T.; Tiziano, F. D.; Cifuentes-Diaz, C.; Miniou, P.; Roblot, N.; Dierich, A.; Le Meur, M.; Melki, J. Nuclear targeting defect of SMN lacking the C-terminus in a mouse model of spinal muscular atrophy. *Hum. Mol. Genet.* **2000**, *9*, 849–858.
- Hsieh-Li, H. M.; Chang, J. G.; Jong, Y. J.; Wu, M. H.; Wang, N. M.; Tsai, C. H.; Li, H. A mouse model for spinal muscular atrophy. *Nat. Genet.* **2000**, *24*, 66–70.
- Monani, U. R.; Sendtner, M.; Covert, D. D.; Parsons, D. W.; Andreassi, C.; Le, T. T.; Jablonka, S.; Schrank, B.; Rossol, W.; Prior, T. W.; Morris, G. E.; Burghes, A. H. M. The human centromeric survival motor neuron gene (*SMN2*) rescues embryonic lethality in *Smn*^{0/0} mice and results in a mouse with spinal muscular atrophy. *Hum. Mol. Genet.* **2000**, *9*, 333–339.
- Butchbach, M. E. R.; Burghes, A. H. M. Perspectives on models of spinal muscular atrophy for drug discovery. *Drug Discovery Today: Dis. Models* **2004**, *1*, 151–156.
- Le, T. T.; Pham, L. T.; Butchbach, M. E. R.; Zhang, H. L.; Monani, U. R.; Covert, D. D.; Gavrilina, T. O.; Xing, L.; Bassell, G. J.; Burghes, A. H. M. SMNΔ7, the major product of the centromeric survival motor neuron (*SMN2*) gene, extends survival in mice with spinal muscular atrophy and associates with full-length SMN. *Hum. Mol. Genet.* **2005**, *14*, 845–857.
- Monani, U. R.; Pastore, M. T.; Gavrilina, T. O.; Jablonka, S.; Le, T. T.; Andreassi, C.; DiCocco, J. M.; Lorson, C.; Androphy, E. J.; Sendtner, M. A transgene carrying an A2G missense mutation in the SMN gene modulates phenotypic severity in mice with severe (type I) spinal muscular atrophy. *J. Cell Biol.* **2003**, *160*, 41–52.
- Andreassi, C.; Angelozzi, C.; Tiziano, F. D.; Vitali, T.; De Vincenzi, E.; Boninsegna, A.; Villanova, M.; Bertini, E.; Pini, A.; Neri, G.; Brahe, C. Phenylbutyrate increases SMN expression in vitro: relevance for treatment of spinal muscular atrophy. *Eur. J. Hum. Genet.* **2004**, *12*, 59–65.
- Andreassi, C.; Jarecki, J.; Zhou, J.; Covert, D. D.; Monani, U. R.; Chen, X.; Whitney, M.; Pollok, B.; Zhang, M.; Androphy, E.; Burghes, A. H. M. Aclarubicin treatment restores SMN levels to cells derived from type I spinal muscular atrophy patients. *Hum. Mol. Genet.* **2001**, *10*, 2841–2849.
- Brichta, L.; Hofmann, Y.; Hahnen, E.; Siebzehrnubel, F. A.; Raschke, H.; Blumcke, I.; Eyupoglu, I. Y.; Wirth, B. Valproic acid increases the *SMN2* protein level: a well-known drug as a potential therapy for spinal muscular atrophy. *Hum. Mol. Genet.* **2003**, *12*, 2481–2489.

- (31) Chang, J. G.; Hseih-Li, H. M.; Jong, Y. J.; Wang, N. M.; Tsai, C. H.; Li, H. Treatment of spinal muscular atrophy by sodium butyrate. *Proc. Natl. Acad. Sci. U.S.A.* **2001**, *98*, 9808–9813.
- (32) Sumner, C. J.; Huynh, T. N.; Markowitz, J. A.; Perhac, J. S.; Hill, B.; Coovert, D. D.; Schussler, K.; Chen, X.; Jarecki, J.; Burghes, A. H. M.; Taylor, J. P.; Fischbeck, K. H. Valproic acid increases SMN levels in spinal muscular atrophy patient cells. *Ann. Neurol.* **2003**, *54*, 647–654.
- (33) Jarecki, J.; Chen, X.; Bernardino, A.; Coovert, D. D.; Whitney, M.; Burghes, A.; Stack, J.; Pollok, B. A. Diverse small-molecule modulators of SMN expression found by high-throughput compound screening: early leads towards a therapeutic for spinal muscular atrophy. *Hum. Mol. Genet.* **2005**, *14*, 2003–2018.
- (34) Harris, N. V.; Smith, C.; Bowden, K. Antifolate and antibacterial activities of 5-substituted 2,4-diaminoquinazolines. *J. Med. Chem.* **1990**, *33*, 434–444.
- (35) Hynes, J. H.; Tomazic, A.; Parrish, C. A. Further studies on the synthesis of quinazoline from 2-fluorobenzonitriles. *J. Heterocycl. Chem.* **1991**, *28*, 1357–1363.
- (36) Nettles, S. M.; Matos, K.; Burkhardt, E. R.; Rouda, D. R.; Corella, J. A. Role of NaBH₄ stabilizer in the oxazaborolidine-catalyzed asymmetric reduction of ketones with BH₃–THF. *J. Org. Chem.* **2002**, *67*, 2970–2976.
- (37) A similar trend was also observed with couple of other sulphides and sulphones. In addition, in vitro metabolic stability studies using rat and human liver microsomal preparation revealed that the thioethers disappeared rapidly, most likely because of oxidation at sulfur to provide sulfoxide and/or sulphone.
- (38) For conformational analysis the (S)-enantiomer of analogues **7a**, **9a** and **9b** were used using Systematic Search sub-routine of SYBYL.
- (39) SYBYL Molecular Modeling Systems, versions 6.9 and 7.0; Tripos Associates: St. Louis, MO.
- (40) (a) Cockerell, G. L.; McKim, J. M.; Vonderfecht, S. L. Strategic importance of research support through pathology. *Toxicol. Pathol.* **2002**, *30* (1), 4–7. (b) McKim, J. M.; Wilga, P. C.; Pregenzer, J. F.; Petrella, D. K. A biochemical approach to in-vitro toxicity testing. *Pharm. Discovery* **2005**, *1*, 30–36.
- (41) (a) McGuir, J. J. Anticancer antifolates: current status and future directions current pharmaceutical design. *Curr. Pharm. Des.* **2003**, *9* (31), 2593–2613. (b) Moffatt, B. A.; Ashihara, H. Purine and pyrimidine nucleotide synthesis and metabolism. *Arabidopsis Book* **2002**, *39* (1), 1–20.
- (42) Cody, V.; Luft, J. R.; Walt, P.; Gangjee, A.; Queener, S. F. Structure determination of tetrahydroquinazoline antifolates in complex with humane and *Pneumocystis carinii* dihydrofolate reductase: correlations between enzyme selectivity and stereochemistry. *Acta Crystallogr.* **2004**, *D60*, 646–655.
- (43) Analogues representing this approach will be reported in a future communication elsewhere.
- (44) It is worth pointing out that during the docking studies for some selected analogues corresponding to the reverse benzyl ether series (**10**) using the DHFR active site (using coordinates of 1s3u.pdb), an intramolecular hydrogen bond was observed between the benzyl ether oxygen and HN of the 4-amino group instead of the typical H-bond of N4–H with Val115 carbonyl. However, this in silico observation has not been confirmed with experimental data.
- (45) Ashton, W. T.; Hynes, J. B. Synthesis of 5-substituted quinazolines as potential antimalarial agents. *J. Med. Chem.* **1973**, *16*, 1233.
- (46) (a) Zlokarnik, G. Fusions to beta-lactamase as a reporter for gene expression in live mammalian cells. *Methods Enzymol.* **2000**, *326*, 221–244. (b) Zlokarnik, G.; Negulescu, P. A.; Knapp, T. E.; Mere, L.; Burres, N.; Feng, L.; Whitney, M.; Roemer, K.; Tsien, R. Y. Quantitation of transcription and clonal selection of single living cells with β -lactamase as reporter. *Science* **1998**, *279*, 84–88.
- (47) Appleman, J. R.; Howell, E. E.; Kraut, J.; Kuhl, M.; Blakley, R. L. *J. Biol. Chem.* **1988**, *263*, 9187–9198.
- (48) Coovert, D. D.; Le, T. T.; McAndrew, P. E.; Strasswimmer, J.; Crawford, T. O.; Mendell, J. R.; Coulson, S. E.; Androphy, E. J.; Prior, T. W.; Burghes, A. H. M. The survival motor neuron protein in spinal muscular atrophy. *Hum. Mol. Genet.* **1997**, *6*, 1205–1214.
- (49) Young, P. J.; Le, T. T.; Thi Man, N.; Burghes, A. H. M.; Morris, G. E. The relationship between SMN, the spinal muscular atrophy protein, and nuclear coiled bodies in differentiated tissues and cultured cells. *Exp. Cell Res.* **2000**, *25*, 365–374.
- (50) Butchbach, M. E. R.; Guo, H.; Lin, C. G. Methyl- β -cyclodextrin but not retinoic acid reduces EAAT3-mediated glutamate uptake and increases GTRAP3-18 expression. *J. Neurochem.* **2003**, *84*, 891–894.

JM061475P